WHITE PAPER

MARCH 2022

OPPORTUNITIES AND RISKS FOR A NATIONAL LOW-CARBON FUEL STANDARD

Nikita Pavlenko, Stephanie Searle, and Adam Christensen (GAMS)

www.theicct.org

communications@theicct.org

twitter @theicct

GAMS

BEIJING | BERLIN | SAN FRANCISCO | SÃO PAULO | WASHINGTON

THE INTERNATIONAL COUNCIL ON CLEAN TRANSPORTATION

ACKNOWLEDGMENTS

This study was generously supported by the David and Lucile Packard Foundation. Thanks to Jeremy Martin of the Union of Concern Scientists and Colin Murphy of University of California, Davis for providing helpful reviews.

Edited by Amy Smorodin

International Council on Clean Transportation
1500 K Street NW, Suite 650
Washington, DC 20005

communications@theicct.org | www.theicct.org | @TheICCT

TABLE OF CONTENTS

ABBREVIATIONS

CFS	Clean Fuel Standard
CNG	Compressed natural gas
CO_2e	Carbon dioxide equivalents
EV	Electric vehicle
FOGs	Fats, oils, and greases
GGE	Gallons gasoline-equivalent
GHG	Greenhouse gas
HDV	Heavy-duty vehicle
HVO	Hydrotreated vegetable oil
ICE	Internal combustion engine
ILUC	Indirect land-use change
LCA	Life-cycle assessment
LCFS	Low Carbon Fuel Standard
LDV	Light-duty vehicle
MJ	Megajoule
MSW	Municipal solid waste
MtCO_2e	Million tonnes CO_2-equivalents
RFS	Renewable Fuel Standard
UCO	Used cooking oil
VMT	Vehicle miles traveled
ZEV	Zero-emission vehicle

EXECUTIVE SUMMARY

This study assesses the economic and environmental impacts of replacing the federal Renewable Fuels Standard (RFS) with a national low-carbon fuel standard (LCFS). The current RFS mandates the blending of a set quantity of biofuels each year, primarily encouraging the use of first-generation biofuels such as corn ethanol and soy biodiesel. A national LCFS has been proposed by some stakeholders as a means of achieving greater GHG reductions from the transport sector, as it would credit fuels proportionally to their life-cycle greenhouse gas (GHG) savings, be technology-neutral, and incentivize efficiency improvements for biofuel production. Key considerations for a national LCFS are the contribution of indirect land-use change (ILUC) to GHG emissions and the sustainability impacts of crop-based fuels that compete with food for limited cropland, which can threaten to undermine emissions savings. Second-generation fuel pathways, which utilize lignocellulosic wastes and residues, can theoretically deliver greater carbon savings with lower land-use impacts, but have thus far struggled to commercialize under the RFS.

In order to assess the potential GHG and economic impacts of moving from the RFS to a national LCFS, we estimated the future mix of fuels supplied to the transport sector under various LCFS implementation scenarios for the period 2020 through 2035. These nine LCFS scenarios include three GHG reduction targets, three different assessments of indirect land-use change (ILUC) impacts, and three different safeguards to cap the contributions of certain fuels:

» Scenario 1: 13% GHG savings by 2035, EPA RFS ILUC emission factors

» Scenario 2: 20% GHG savings by 2035, EPA RFS ILUC emission factors

» Scenario 3: 27% GHG savings by 2035, EPA RFS ILUC emission factors

» Scenario 4: 27% GHG savings by 2035, post-hoc ILUC adjustment with higher ILUC emissions

» Scenario 5: 18.6% GHG savings by 2035, high ILUC factors

» Scenario 6: 28.3% GHG savings by 2035, California LCFS ILUC factors

» Scenario 7: 16.7% GHG savings by 2035, EPA RFS ILUC emission factors; separate caps for food-based biofuels and waste-oil derived biofuels at 2020 consumption levels

» Scenario 8: 18% GHG savings by 2035, EPA RFS ILUC emission factors; combined cap for food-based biofuels and waste-oil derived biofuels at 2020 consumption levels

» Scenario 9: 21.5% GHG savings by 2035, EPA RFS ILUC emission factors; cap for food-based biofuels at 2020 consumption levels

The results from the scenario analysis are illustrated in Figure ES1 below. As shown, the estimated annual total contribution of ILUC emissions from the average mix of fuels used in on-road transportation in 2035 for each scenario ranges from approximately 6 million to 330 million tonnes CO_2e.

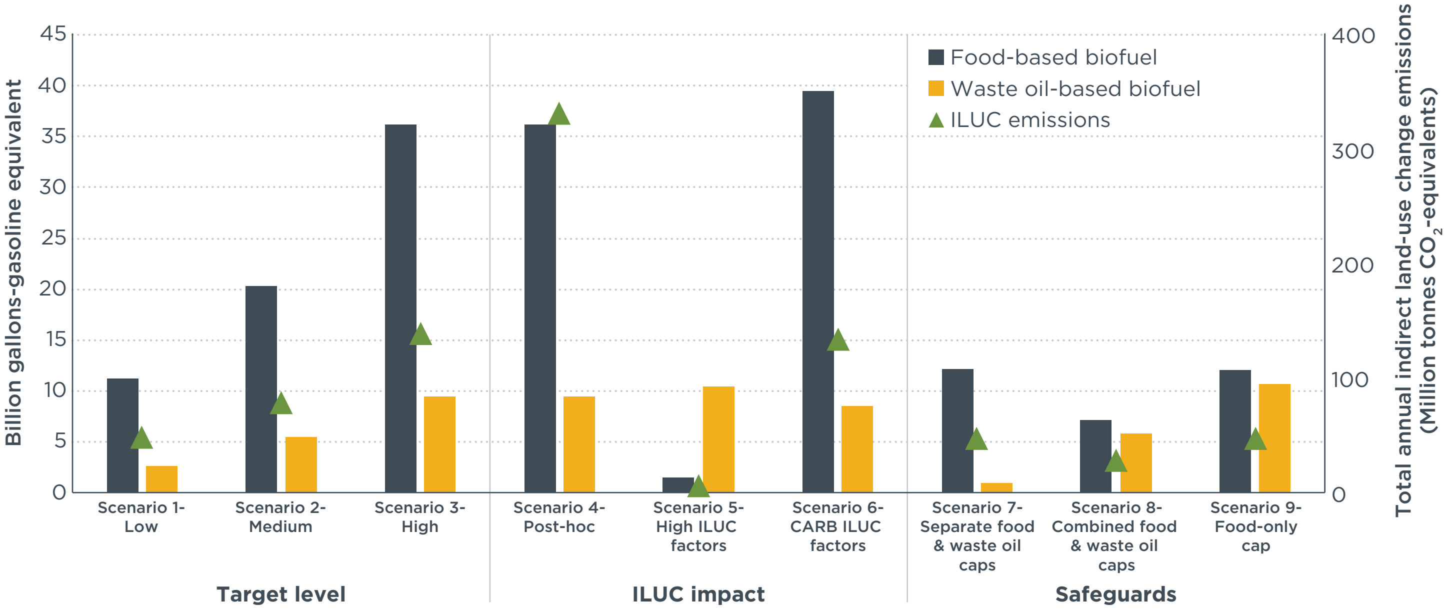

Figure ES1. Projected 2035 volumes of food-based biofuels, waste oil-based biofuels presented alongside total fuel mix ILUC emissions, across multiple LCFS implementation scenarios

Overall, we find that the technology-neutral structure of an LCFS incentivizes emission reductions from existing, commercialized fuel pathways, particularly food-based biofuels and waste oils. However, we find that feedstock specific caps can be used to direct policy support away from riskier feedstocks and towards more challenging, lower-carbon pathways. Our main findings and conclusions are:

A fully technology-neutral national LCFS would greatly increase demand for food-based biofuels. This analysis finds that implementing a fully technology-neutral, national-level LCFS similar to existing state-level policies would greatly increase the incentive for food-based biofuel production. In scenarios without any restrictions on the contribution of food-based biofuels (Scenarios 1–4 and 6), we find that the consumption of food-based biofuels production increases up to 220% relative to 2020 levels.

A national LCFS may induce a substantial increase in waste oil imports with sustainability risks. True waste oils are a highly constrained resource that is strongly incentivized by the LCFS design. The United States has already begun exhausting domestic resources and importing these feedstocks from Asia. There are widespread concerns that this imported oil may be virgin palm or other vegetable oils fraudulently claimed as waste oils. We estimate that without safeguards, waste oil biofuel volumes would increase by as much as 10 times, as shown in Figure ES-1. This quantity cannot plausibly be supplied by genuine waste oil collection in Asia. We find that waste oil fraud could increase the GHG emissions of the average fuel mix by up to 5%, depending on the scenario, and reduce the intended GHG savings from the LCFS by up to 4%.

Uncertainty in indirect land-use change emissions accounting may reduce the *de facto* GHG savings from an LCFS. The indirect land-use change emissions associated with crop-based biofuels are highly uncertain, but may be high enough from some crops to reduce or even entirely undermine their emissions savings relative to fossil fuels. Even when ILUC accounting is included in an LCFS, there is a high risk of underestimating these impacts, which may incentivize riskier pathways. By assessing the post-hoc potential impact of higher ILUC emissions on the mix of fuels supplied in the high target level scenario (Scenario 4), we estimate that the average carbon intensity of fuels would be an additional 10.1 gCO_2e/MJ higher, reducing the *de facto* GHG savings from the policy by over 40%.

Separate caps on food-based biofuels and waste oils are effective in limiting the ILUC risk of a national Clean Fuels Standard. We find that introducing these safeguards results in a lower GHG reduction target, but with much higher integrity than the corresponding technology-neutral scenario. All three safeguard scenarios have total ILUC emissions below 50 million tonnes in 2035, roughly one-third of those in the corresponding high target scenario without any safeguards. We find that a separate cap for waste oils is necessary to prevent fraudulent use of virgin palm oil. Even when uncertainty in ILUC emissions and used cooking oil fraud-risk emissions are taken into account, the carbon intensity of the fuel mix in this scenario would only be 1% higher than the GHG target if regulators underestimate ILUC. We also find that implementing dual caps better supports the development of a sustainable and scalable second-generation cellulosic biofuel industry, increasing cellulosic biofuel deployment by an additional 300 million GGE relative to the fully technology neutral scenario. Without these specific safeguards, we find there is a high risk that a national LCFS would not deliver the level of GHG reductions nor advance the second-generation biofuels industry necessary for deep decarbonization of the U.S. transport sector.

Transitioning from the existing federal RFS to a national LCFS necessitates a large-scale restructuring of U.S. fuel policy. It is therefore critical to evaluate the potential climate benefits of an LCFS and whether they justify the legislative and regulatory effort to overturn and replace the existing Renewable Fuel Standard (RFS).

INTRODUCTION

The lack of Congressionally-mandated volumes for the federal Renewable Fuels Standard (RFS) after 2022 creates a substantial political opportunity to re-evaluate U.S. fuels policy; while the U.S. Environmental Protection Agency (EPA) will have the authority to set volume mandates from 2023 onward, it will have greater discretion on how to administer the program. The uncertainty over the future of the RFS program after 2022, as well as concerns over its effectiveness at reducing GHG emissions, have prompted interest in its replacement by members of Congress, industry stakeholders, and some academics (House Select Committee on the Climate Crisis, 2020; Kelly & Renshaw, 2020; Sperling et al., 2020). These stakeholders have proposed the implementation of a national low-carbon fuel standard (LCFS), based on state-level programs such as California's LCFS and Oregon's Clean Fuels Program (CFP), as a possible replacement for the federal RFS. This paper evaluates the GHG reduction potential of implementing a hypothetical national LCFS, assesses the risks of that proposal, and explores the effect of policy safeguards to ensure the integrity of emission reductions.

While the RFS mandates a certain volume of fuels each year, with sub-targets for different biofuel categories, an LCFS mandates a reduction in the average carbon intensity (CI) of fuels supplied to the transport sector. This greenhouse gas (GHG) target is assessed based on the average CI of the fuels supplied to the transport sector.[1] A carbon intensity standard follows a declining CI target for each year; fuels above the target generate deficits based on their CI, and fuels below the target generate credits proportional to their difference from the standard, as shown in Figure 1 below. Obligated parties such as oil refiners and suppliers must blend alternative, low-CI fuels or acquire credits to ensure that they offset their deficits. Carbon intensity standards offer several advantages compared to a volumetric mandate like the RFS. They are technology-neutral and allow non-biomass energy sources such as grid mix electricity to charge electric vehicles, renewable electricity, and green hydrogen to generate credits. They also incentivize continuous improvement in fuel production efficiency because facilities that reduce their GHG emissions generate more credits. In addition, CI standards incentivize different types of alternative fuels proportionally to their GHG savings.

1 In this section we use the more general term "carbon intensity standard" to describe other jurisdictions' policies—otherwise, we use the term LCFS.

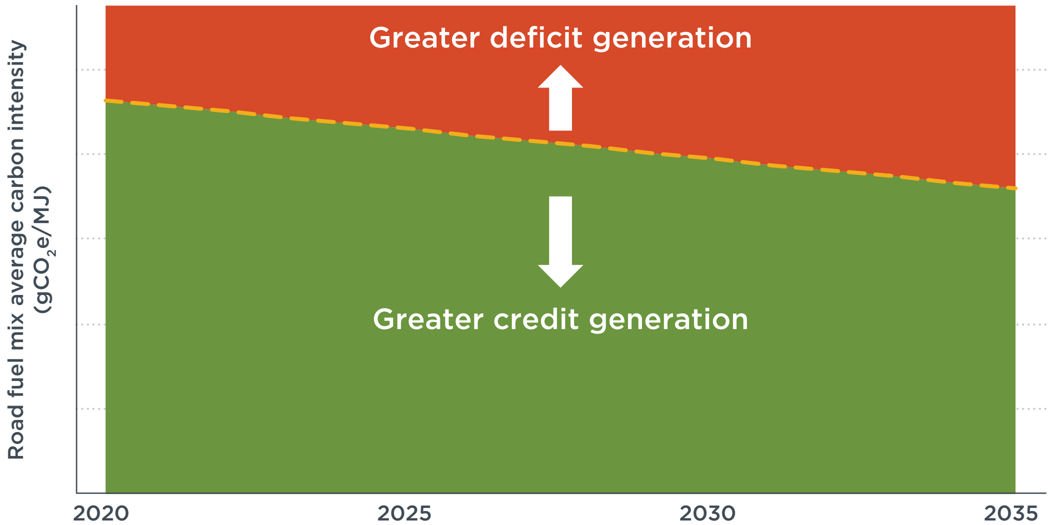

Figure 1. Example of declining average road sector average carbon intensity implemented over time

Fuel CI standards have already been implemented or are in the process of being implemented in multiple state-level jurisdictions throughout the United States. California was the first U.S. state to do so, implementing an LCFS beginning in 2011, and the standard has been recently recertified and extended to a 20% CI reduction for its transport fuel mix by 2030 (17 CCR § 95482). California's LCFS was followed by Oregon's Clean Fuels Program, which mandates a 10% fuel CI reduction in by 2025, and Washington State, which established a 20% CI reduction target for 2035 (Oregon DEQ, 2021; Reducing Greenhouse Gas Emissions by Reducing the Carbon Intensity of Transportation Fuel, 2021). Similar policies have been developed outside the United States, such as British Columbia's Renewable and Low Carbon Fuel Requirement Regulation (RLCFRR), Brazil's RenovaBio program, and Canada's forthcoming federal Clean Fuel Standard (BC Reg 394/298; Canada Gazette Part I, Volume 154, Number 51; Lei Ordinária 13.576, de 26.12.2017). The EU established a carbon intensity performance standard in its Fuel Quality Directive, requiring a 6% reduction in GHG emissions for EU road transport fuel by 2020 compared to 2010 (EU Directive 2009/30/EC), and has proposed a new 13% GHG intensity reduction target for the total transport sector in 2030 as part of the proposed revision to Renewable Energy Directive (European Commission, COM/2021/557 final).

The carbon intensity of different transport fuels within fuel standards is typically determined using a life-cycle assessment (LCA) to estimate a fuel's well-to-wheel GHG emissions. The results are typically presented using a standardized, harmonized metric in order to compare different types of fuels on a consistent basis (i.e., CO_2-equivalents per MJ of delivered energy).[2] A large component of the lifecycle GHG emissions of crop-based biofuel pathways is induced land-use change (ILUC). Induced land-use change occurs when the increased demand for an agricultural commodity results in direct or indirect cropland expansion to compensate for the shortfall in supply. These emissions are generally estimated using economic models. While the magnitude of ILUC emissions is uncertain, it is generally understood to be

2 For fuels using different drivetrains, such as electricity used in electric vehicles, or hydrogen used in fuel cell vehicles, GHG assessments include an energy economy ratio (EER) to account for differences in efficiency between different vehicle types

large enough to substantially reduce or negate the carbon savings from the use of biofuels (Woltjer et al., 2017). The efforts to develop LCA factors for alternative fuels for the Carbon Offsetting and Reduction Scheme for International Aviation (CORSIA) highlights the difficulty of achieving both consensus and certainty on ILUC emissions; when comparing ILUC emission results from two economic models with harmonized assumptions, they were as far apart as 95.4 gCO_2e/MJ for some pathways—for reference, the lifecycle GHG intensity of petroleum-based kerosene in CORSIA is 89 gCO2e/MJ (ICAO, 2019). Plevin et al. (2015) suggests that the wide uncertainty range for estimating ILUC emissions makes LCFSs that rely on them an inherently risky policy design.

While technology-neutrality is an important component of performance standards, in practice, it has hindered the deployment of ultra-low carbon and zero-emission fuels in favor of cheaper food-based biofuels and waste oils. California's LCFS, thus far, has failed to increase the deployment of second-generation, lignocellulosic biofuels, even as the CI target has continued to decline. In California, cellulosic ethanol is a minor contributor to the program, reaching only 91 million gasoline-gallon equivalents, or 5% of alternative fuels consumed, in 2019 (CARB, 2021).[3] Bushnell et al. (2020) speculate that in the absence of widespread vehicle electrification or carbon capture and sequestration, the primary mode of compliance for California's LCFS would come from a substantial increase in biomass-based diesel, reaching up to 60% of California's total diesel consumption.

Waste oils are a scarce resource; researchers have estimated that the United States already collects more than 80% of its potential used cooking oil (GreenEa, 2021) and the overall domestic availability of waste oils and fats for biofuel production in the United States is likely to decline in future years (Zhou et al., 2020). High incentives for used cooking oil biofuel in the European Union have led to cases of virgin vegetable oil being fraudulently claimed as used cooking oil (Court of Rotterdam, 2020; European Anti-Fraud Office, 2019) and there are widespread concerns that such fraud may be rampant and largely undetected (van Grinsven et al., 2010). Because an LCFS design rewards waste oil-based compared to crop-based biofuels, there is a risk that, after exhausting the domestic supply of genuine used cooking oil, such a policy would drive fraudulent imports.

A California Air Resources Board staff review of the state's LCFS in 2011 noted that, "If the development of [ultralow carbon] fuels in sufficient volumes does not occur under the current structure of the LCFS (based on the need for regulated parties to comply with the LCFS), special provisions within the regulation may aid in their development" (Corey et al., 2011). Alternatives to a fully technology-neutral LCFS, such as caps on the contribution of some feedstocks or additional incentives for more challenging fuel pathways, may be necessary to increase the role of these fuels. This is not without precedent: in 2019, California added an additional credit-generation incentive for direct current (DC) fast charging stations for electric vehicles to support their deployment (17 CCR § 95482).

While existing policies have provided a broad template for how to structure an LCFS, policymakers still have many decisions to make on how a future LCFS policy could be implemented at the national level. Key considerations include how high to set targets and whether to use a carbon accounting framework that is different from

3 Ethanol derived from residue in California may also include non-cellulosic feedstocks such as waste wine

both the EPA's existing RFS and the state-level LCFSs. In this study, we assess the impact of several policy design choices for a hypothetical national LCFS and evaluate their impact on the overall climate impact of the policy and the mix of alternative fuels deployed through the program. Using an economic model, we evaluate several different LCFS scenarios through 2035.

METHODOLOGY

MODEL DESIGN

For our analysis, we utilize a model of the U.S. transportation fuel market developed in the GAMS modeling language. The model is a partial equilibrium model. We developed our baseline reference data from various data sources described in the subsequent section and in more detail in Appendix A.

Calibration was verified and counterfactual policy scenarios (i.e., policy shocks) were developed to gauge the market response; each scenario has different GHG reduction targets, fuel eligibilities, and LCA factors, as described in the next section. The transportation market has several different agents that make rational economic decisions based on information that they can access. The model contains representative consumers, a blender agent, and supply agents for different blendstock fuels. Details of each of these agent problems are provided in the following sections.

We use the Extended Mathematical Programming (EMP) syntax to reformulate the collection of agent optimization problems (or their first order or KKT conditions) into a single complementarity model Ferris et al. [1]. The model is ultimately solved with the PATH algorithm.

Consumer Agents

There are two classes of consumer in this model: 1) a light-duty vehicle (LDV) consumer and 2) a heavy-duty vehicle (HDV) consumer. Both consumer agents are modeled as cost minimizers that make vehicle purchase designs based on the cost of vehicles and the cost of vehicle miles traveled (VMTs) across several different vehicle categories. The LDV consumer can purchase gasoline LDVs, diesel LDVs, or electric vehicles. The HDV consumer can purchase diesel HDVs, compressed natural gas (CNG) HDVs, or hydrogen fueled HDVs.

The production of VMT by these vehicle classes is modeled by a constant elasticity of substitution (CES) style production function. The CES style production function allows for vehicle preferences to change between categories and is used to capture the aggregate preferences for all consumers, economy-wide; we utilize the calibrated share form of the CES function as described by Rutherford (2002). The consumer agent problem can be described mathematically as the following optimization problem (Equation 1).

Equation 1. Consumer agent optimization

$$\min_{VKTv} \sum_{v,f} \left[\frac{(P_f - P_f^{LCFS})}{\gamma_v} + Z_v^{opex} + Z_v^{capital} \right] VMT_v$$

$$\text{s.t.} \sum_{v} \left[\theta_v \left(\frac{VMT_v}{\overline{\overline{VMT_v}}} \right)^{\rho} \right]^{1/\rho} = D$$

Where:

$v \varepsilon V$ represents different vehicle technologies

$f \varepsilon F$ represents blended fuels that are used in each vehicle

VMT_v are decision variables that represent the number of miles driven by a vehicle *(billion miles/yr)*

γ_v is the fuel economy of the vehicle *(miles/MJ)*

ρ is the substitution parameter (which is related to the elasticity of substitution)

θ_v is the market value share for vehicle v

Z_v^{opex} is the data that represent non-fuel vehicle operating costs *($/mile)*

$Z_v^{capital}$ is the data that represent vehicle capital costs *($/mile)*

D is the aggregate vehicle market value for an agent *(billion $)*

The final demand is described by an isoelastic function shown in Equation 2 and is a function of the aggregate price index ($P\ D$), which is exactly the dual variable of the CES production function in Equation 1. The aggregate price index is equal to 1 at the benchmark when using the calibrated share form of the CES production function.

Equation 2. Consumer agent final demand equation

$$D = \bar{d}\left(\frac{PD}{1}\right)^{-\varepsilon}$$

Where:

$\bar{d}$ is the baseline aggregate vehicle market value for an agent *(billion $)*

PD is the aggregate price index

ε is the agent's demand elasticity

Blender agent

The model assumes that one blender agent is responsible for all fuel blending and is therefore responsible for providing fuel to the consumer agents that meets all the necessary policy requirements. This single blender replaces, in a modeling context, a group of independent blending agents who would be capable of buying and selling credits in order to meet a carbon standard. Like the consumer agents, the blender agent will blend fuel to minimize costs. The blender agent is assumed to purchase quantities of energy from blendstock suppliers. The blender agent problem can be described mathematically as the base optimization problem shown in Equation 3. The single blender model implies that the price of the LCFS credit is equivalent to the marginal price on the credit market clearing condition in Equation 5 (i.e., zero net credits).

Equation 3. Optimization equation for blender agents

$$\min_{Q_{bs,f}^{blend}} \sum_{bs \varepsilon BSF(bs,f)} \left[Q_{bs,f}^{blend} P_{bs} \right]$$

$$\text{s.t. } P_f = \sum_{bs} \frac{Q_{bs,f}^{blend}}{Q_f} P_{bs}$$

$$Q_f = \sum_{bs} Q_{bs,f}^{blend}$$

$$Q_f = \sum_{v,a} \frac{VMT_{v,a}}{\gamma_v}$$

$$E_f = \frac{\sum_{bs,f} Q^{blend}_{bs,f}}{\sum_{bs',f} \frac{Q^{blend}_{bs',f}}{\rho^{v}_{bs'}}}$$

$$\sum_{bs,bst,f} \frac{\frac{Q^{blend}_{bs',f}}{\rho^{v}_{bs}}}{\frac{Q_f}{E_f}} \leq BLEND^{UP}_{bst,f}$$

$$\sum_{bs,bst,f} \frac{\frac{Q^{blend}_{bs,f}}{\rho^{v}_{bs}}}{\frac{Q_f}{E_f}} \leq BLEND^{LO}_{bst,f}$$

$$\sum_{bs,bst,f} \frac{\frac{Q^{blend}_{bs,f}}{\rho^{v}_{bs}}}{\frac{Q_f}{E_f}} \leq BLEND^{FX}_{bst,f}$$

Where:

$bs \; \varepsilon \; BS$ represents different fuel blendstocks

$f \varepsilon F$ represents blended fuels that are used in each vehicle

$bst \; \varepsilon \; BST$ represents common categories of blendstock types (i.e., all ethanol, all FAME, etc.)

ρ^{v}_{bs} is the energy density of a blendstock *(MJ/physical unit)*

P_f is the final price for blended fuel *($/MJ)*

$Q^{blend}_{bs,f}$ are decision variables that represent the portion of energy from a blendstock used in a finished fuel *(billion MJ)*

Q_f are decision variables that represent the total energy of a finished fuel *(billion MJ)*

E_f are decision variables that represent the energy density of a blended fuel *(MJ/physical unit)*

$BLEND^{LO,UP,FX}_{bst,f}$ are technology-based limits on blending fuels (i.e., E10 blends, etc.)

Policy Constraints

The optimization problem described in Equation 3 describes all the technology-based logic used to define how fuel blending should be performed. Blenders are also subject to a number of policy related constraints that impact blending behaviors in each scenario. We describe each of these formulations separately. If the policy is active in the policy scenario, it is added to the list of technology-based constraints listed in Equation 3. These constraints include limits (in PJ) on the total quantity of food-based biofuels and waste oil-based diesel, and total fuel demand, based on the scenario (the equations for each policy constraint are described in further detail in Appendix B).

The CI standard is included in this model as a policy mechanism for incentivizing alternative fuels and vehicles. Fuels that have a lower EER-adjusted carbon intensity (CI_{bs}) than the standard for a given year will generate credits, and fuels will generate deficits if that fuel has a CI higher than the standard (CI^{std}). The total quantity of credits generated is based on this differential as well as the quantity of fuels for each type supplied to the market (Q_{bs}). Equation 4 dictates how these credits (positive values of Q^{LCFS}) and deficits (negative values of Q^{LCFS}) are generated.

Equation 4. LCFS credit generation equation

$$Q_{bs,f}^{LCFS} = \sum_{std,bs \varepsilon STD(std,bs)} [CI^{std} - CI_{bs}] Q_{bs,f}^{blend}$$

$$P_f^{LCFS} = \sum_{bs,f \varepsilon BSF(bs,f)} \frac{Q_{bs,f}^{blend}}{Q_f} \lambda^{LCFS} [CI^{std} - CI_{bs}] \, Q_{bs,f}^{blend}$$

The price of the LCFS credit each year is the price at which the supply of credit exactly clears the demand for credits. This market clearing condition is described in Equation 5.

Equation 5. LCFS credit market clearance equation

$$\sum_{bs} Q_{bs,f}^{LCFS} = 0$$

Where:

std ε STD represents the different carbon intensity standards

STD(std,bs) represents the two-dimensional set that maps the applicable carbon intensity standard to the blendstock fuel

λ^{LCFS} represents the LCFS credit price (*\$/MTCO$_2$e*)

P_f^{LCFS} represents the final value (cost or benefit) of the LCFS credits associated with a finished (blended) fuel (*\$/MJ*)

The agents that are responsible for supplying blendstocks to the blender are not modeled as individual optimizers. Instead blendstocks are available to the blender through an isoelastic supply curve. This curve is represented by Equation 6.

Equation 6. Blender agent supply curve equation

$$\frac{P_{bs}}{\bar{p}_{bs}} = \frac{Q_{bs}}{\bar{q}_{bs}}^{1/\eta bs}$$

Where:

P_{bs} is the price at which a quantity of blendstock fuel can be supplied *(\$/MJ)*

Q_{bs} is the quantity of blendstock that is demanded under a policy shock *(\$/MJ)*

$\bar{p}_{bs}$ is the baseline price at which the baseline quantity of blendstock that is supplied *(\$/MJ)*

$\bar{q}_{bs}$ is the baseline quantity of blendstock fuel *(\$/MJ)*

η_{bs} is the supply elasticity for a particular blendstock fuel

Credit Banking

The economic optimization approach used in this model can be flexible with respect to how the time dimension is resolved—in particular, the option to generate additional credits in a given year for future use (i.e., credit banking). Of the two agents in the model, only the blender agent passes information between discrete time slices (i.e., variables from *t-1* time slice impact variables in time *t*); the only time dependent decision in this model is the quantity of LCFS credits available to bank and use later.

Rather than a perfect foresight approach, wherein obligated parties view the policy future with 100% certainty and adjust their behavior in the first year of the policy to make compliance in the final year more cost effective, we utilize a moving window, credit banking approach. In this case, blender agents view the policy future as perfectly certain, but only N years into the future instead of perfectly certain across the entire time series of interest. We assume blender agents have a moving time window of 4 years of policy certainty to inform their credit banking decisions.

REFERENCE DATA

This analysis utilizes a counterfactual, business-as-usual transport energy demand scenario based on the U.S. Energy Information Administration (EIA) Annual Energy Outlook's reference scenario, from 2020 through 2035 (EIA, 2020a). We utilize the Annual Energy Outlook projections on energy demand for overall transport fuel broken out into the following subcategories: gasoline, diesel, CNG, electricity, and hydrogen. We also incorporate assumptions of baseline biofuel blending from the Annual Energy Outlook into the baseline scenario, including approximately 5% biodiesel blending and 10.4% ethanol blending (i.e., E10 and a small share of E85 vehicles).[4]

To establish a baseline for alternative fuel usage, we draw upon the U.S. EPA's program data for the RFS, which contains renewable identification number (RIN) generation data broken out by fuel category, RIN type, and feedstock (EPA, 2021). In cases where RIN generation data did not sufficiently disaggregate the mix of feedstocks used to produce the fuels, we supplemented the data with estimates of the feedstock mix for producing fatty acid methyl ester (FAME) biodiesel from the U.S. EIA and estimates of the feedstock mix for producing hydrotreated renewable diesel from CARB.[5]

This analysis uses default emission factors from the GREET 2020 model to estimate the direct emissions for alternative fuels (Wang, et al., 2020). Electricity emissions decline over time based on the mix of electricity in the U.S. grid projected in the U.S. EIA Annual Energy Outlook. For those fuel pathways absent from GREET 2020, we supplement the analysis using values from the literature as described in Appendix A. We utilize EPA's regulatory values for the life-cycle emissions for diesel and gasoline fuels from the RFS (EPA, 2010). To adjust the credit generation from pathways utilizing drivetrains with different energy efficiencies, we utilize the energy efficiency ratios for LDV electric vehicles, hydrogen vehicles, and CNG-powered vehicles in the California LCFS (17 CCR § 95482). This analysis does not factor in any ongoing efficiency improvements for direct biofuel production into the LCA values for fuels.

The ILUC factors for this analysis, shown in Figure 2 below, differ depending on the scenario to illustrate the importance of carbon accounting on the impact of LCFS implementation. Depending on the scenario in question, this analysis adds ILUC emissions for a given feedstock to the direct production emissions for that fuel pathway. For the baseline scenarios, we utilize U.S. EPA's ILUC estimate developed for the RFS for crop-based biofuel pathways, adding together domestic and international

4 This includes a small share of vehicles using higher ethanol blend rates of 15% and 85%, allowing the ethanol blend rate to exceed 10% on a volumetric basis

5 For the renewable diesel category, we assume that the mix of feedstocks is 96% waste-based for California's share of consumption, with the remainder blended outside of California to be food-based

land-use change emissions.[6] To evaluate the impact of higher ILUC values on the implementation and climate impact of the policy, we also assess the impact of higher ILUC factors based on EPA's initial 2009 proposed rulemaking for the RFS for the two largest categories of feedstock, corn and soy (EPA, 2009). Lastly, we include one scenario using California's regulatory ILUC values for biofuels used in the California LCFS (CARB, 2015).[7] For palm oil imported into United States mislabeled as waste oil (i.e., fraudulent waste oil), we use the ILUC factor for palm oil developed by CARB of 71.4 gCO_2e/MJ (CARB, 2015).

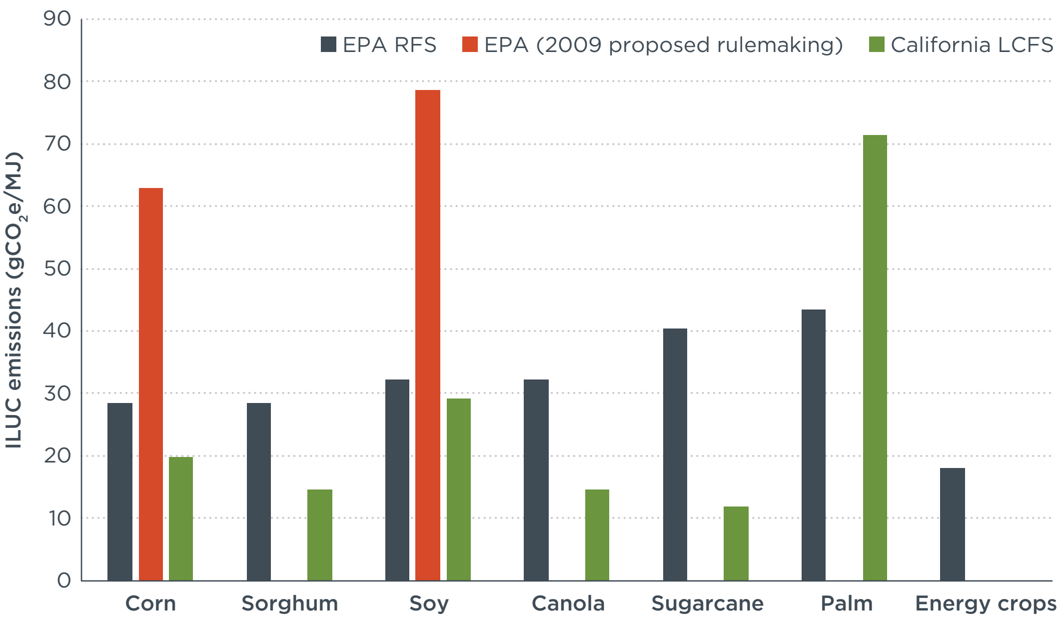

Figure 2. Comparison of ILUC factors used in this analysis

To assess the risk of waste oil fraud, we first determine a plausible upper bound for waste oil imports. Zhou et al. (2020) estimate that there is little room for growth in the domestic supply of waste fats, oils, and greases in the United States through 2032; the authors find that these feedstocks are already largely utilized, and their availability will decline by 8% from 2020 through 2032. Consequently, additional demand for waste oils is expected to be met through increased imports from Asia, based on existing trends from biofuel policy compliance in California and the European Union (Zhou et al., 2020; GreenEA, 2021). To quantify waste oil availability, we sum the total used cooking oil consumption in major Asian markets for 2035 based on FAOStat projections, including China, South Korea, Malaysia, Indonesia, and India (FAOStat, 2021). To determine the share of used cooking oil collection that is feasible, we assume a loss rate of 50% and then a collection rate of 5%. This collection rate is based on an analysis in Indonesia of the share of total used cooking oil (UCO) potential that is at easily collectable sites, such as industrial sites, urban restaurants, and schools (Kharina et al., 2018). This quantity would produce approximately 1 billion GGE of renewable diesel. We also consider a more optimistic collection rate, based on an analysis by India's Food Safety and Standards Authority (FSSAI), which would entail the full collection of the waste fraction of used cooking oil at industrial sites

6 In the absence of ILUC factors for these feedstocks in the original assessment, we assume ILUC values for sorghum and canola equivalent to corn and soy, respectively.

7 For the CARB ILUC scenario, we assume ILUC emissions are 0 gCO_2e/MJ for lignocellulosic energy crops such as switchgrass and miscanthus

and restaurants, in conjunction with collection of 15% of all household UCO, which would yield approximately 5 billion GGE of waste oil-derived biofuels in Asia (FSSAI, 2019). We assume that any supply of UCO beyond these quantities would come from fraudulently mislabeled virgin vegetable oils, particularly low-cost palm oil produced in Southeast Asia. We then apply a palm oil ILUC emission factor to that share of the fuel mix, increasing the net emissions of these fuels to reflect the emissions attributable to waste oil fraud.

To evaluate the cost-optimized mix of fuels to meet the GHG reduction target, we incorporate wholesale and taxed fuel prices into the model for each fuel. Fossil fuel prices are based on the five-year wholesale average reported to EIA (EIA, 2020b). First-generation biofuel prices are compiled based on the last five years of market data; advanced biofuel prices are estimated based on techno-economic assessments in the literature as described in Appendix A. Given that electric vehicle charging occurs both at residences and at higher-cost, public fast charging sites, we develop a weighted average electricity cost that assumes a mix of 80% home charging, 15% public Level 2 charging, and 5% public fast charging (Francfort, 2015). For public fast charging, we incorporate charging infrastructure cost estimated by Nicholas (2019).

The consumer agent module for the model incorporates a degree of vehicle switching for consumers in response to the LCFS; therefore, we incorporate generalized vehicle cost, VMT, and fuel economy data for several broad vehicle categories. For the LDV fleet, we incorporate projections of year-over-year declines in electric vehicle costs as estimated by Lutsey and Nicholas (2019). For the HDV fleet, we assume efficiency increases and cost increases for conventional, diesel-powered tractor-trailers over the period assessed, with corresponding cost declines in alternative fuel tractor-trailers powered by CNG or hydrogen (Moultak et al., 2017).

For this analysis, we assume that electric vehicle deployment is encouraged through complementary policies outside of the LCFS, including zero-emission vehicle (ZEV) mandates, efficiency standards, and direct incentives such as ZEV rebates. Therefore, we utilize an adjusted reference case for EV deployment and the quantity of electricity consumed by the LDV fleet. We assume that the electric vehicle sales share of LDV's increases from 1% in 2020 to 2% in 2025, accelerating to 25% in 2030 and 70% in 2035. We then use a fleet turnover model developed by Lutsey (2015) to estimate the electricity demand from the additional electric vehicle deployment relative to increase projected in the EIA Annual Energy Outlook. Based on these projections, we estimate that electric charging for the LDV fleet will increase to approximately 685 PJ of electricity (approximately 5.8 billion GGE) in 2035. To compensate for this increase in electric charging, we subtract an equivalent, EER-adjusted quantity of gasoline-pool fuel demand from the EIA reference scenario. Similar to provisions for residential charging revenue in the California LCFS, we assume that the credit revenue generated by electric vehicle charging in the LCFS modeled here feeds into the consumer agent module of the model; here, LCFS revenue reduces the cost of electric vehicle acquisition and use.

SCENARIO DESIGN

This analysis uses three categories of scenarios to test three separate aspects of LCFS design, as illustrated below in Table 1, for a total of nine scenarios. The table illustrates the high-level design considerations for each scenario, including the credit price range, GHG reduction target, the choice of ILUC factors, and whether there are any caps on contributions from specific feedstocks.

Table 1. Overview of LCFS modeling scenarios and parameters

Scenario name	Category	Credit price	GHG reduction target	ILUC factors	Feedstock caps
1 – Low	Target level	Low	13.0%	EPA RFS	No
2 – Medium		Medium	20.0%	EPA RFS	No
3 – High		High	27.0%	EPA RFS	No
4 – Post-hoc ILUC	ILUC impact	High	27.0%	EPA RFS (post-hoc EPA 2009 adjustment)	No
5 – High ILUC factors		High	18.5%	EPA 2009	No
6 – CARB ILUC factors		High	28.3%	CARB LCFS	No
7—Separate caps	Safeguards	High	16.7%	EPA RFS	Separate caps for food-based biofuels and waste oils
8 – Combined cap		High	18.0%	EPA RFS	Combined for food-based biofuels and waste oils
9 – Food-only cap		High	21.5 %	EPA RFS	Cap on food-based biofuel only

For the first set of three scenarios, we investigate three different GHG reduction target levels. We identify these target levels by targeting credit price caps under varying levels of climate ambition: \$250, \$450, and \$650 per tonne CO_2e. Working backwards from the three assumed credit price caps, we use the model to calibrate the 2035 GHG reduction targets that would result in these credit prices, arriving at 13%, 20%, and 27% for the three scenarios. This set of scenarios do not include any restrictions on feedstock contributions to the overall policy target and uses EPA's current emission factors for ILUC emissions under the RFS.

Scenarios 4 through 6 use different ILUC factors to assess the climate risk of inaccurate carbon accounting in an LCFS policy. All three scenarios in this category are based on a "high" credit price level of \$650 per tonne CO_2e, with the GHG reduction targets differing from the previous set of scenarios based on changes in the compliance costs due to differences in the CI of some feedstocks. Scenario 4 assesses the risk of understating ILUC emissions by modeling identical target levels and fuel CI's as Scenario 3; however, we adjust the emissions *post-hoc* using ILUC factors from EPA's 2009 proposed rulemaking for corn and soy to assess the difference between the modeled CI reduction and emissions savings and the hypothetical, *de facto* emissions reduction from the fuel mix. Scenario 5 utilizes ILUC factors from EPA's 2009 RFS proposed rulemaking within the modeled CI scores for fuels, which significantly increases the well-to-wheel emissions for soy- and corn-derived fuels. Scenario 6 uses the ILUC values estimated by CARB for the LCFS in 2015, which are similar to those used in the EPA RFS and thus result in a similar GHG reduction target to Scenario 3.

Scenarios 7 through 9 explore the impact of adding safeguards in the form of feedstock-based caps to LCFS compliance. In these scenarios, the contribution of either food-based biofuels or waste oil-derived biofuels is capped on an energy basis to the total quantity of fuel consumed in the transport sector. We assume a "high" credit price of \$650 per tonne and estimate the GHG reduction target for each scenario, which ranges from 16.7% in Scenario 7 to 21.5% in Scenario 9; these targets are lower than the other high ambition scenarios due to the feedstock caps, which necessitate greater use of more expensive advanced fuels and thus a lower overall target to stay within designated price range. The feedstock caps are based on 2019 consumption levels derived from EPA RFS RIN data for both total food-based biofuel consumption, 12.1 billion gallons of gasoline-equivalents (GGE), and the total amount of waste oil-derived biofuels, 0.9 billion GGE. For the latter, this category includes used cooking oil, corn oil, and inedible animal fats. We evaluate three types of energy-based caps: a food-based biofuels-only cap, a combined food and waste oil-derived biofuels cap, and lastly, separate caps for both categories. In each case, the cap is implemented separately from the CI target for the LCFS and is instead modeled similarly to a blending limit. Within the cap, the mix of feedstocks and fuels can change significantly in response to the policy targets and deliver different CI reductions. For example, conventional corn ethanol use may decline in favor of additional soy renewable diesel use so long as their combined total does not exceed the limit.

SCENARIO RESULTS

Here, we present the results of each of the nine scenarios modeled.

COMPARING THE IMPACT OF GHG REDUCTION TARGETS

Scenario 1, illustrated in Figure 3a, represents a case in which an LCFS implements a 13% reduction in average CI for the transport fuel mix by 2035. Each component of the stacked chart area illustrates the contribution of that fuel category in billion GGE to the overall transport fuel mix over the time period assessed. This scenario has the lowest GHG reduction target of any scenario in this analysis, but still prompts changes in the transport fuel mix; though ethanol consumption declines over the time period due to declining gasoline demand and the E10 blend wall, renewable diesel production from soy and waste oils increases significantly starting in 2025. Though electric charging increases over the time period, the growth is primarily attributable to complementary policies such as ZEV mandates and incentives in the reference scenario; we find there is only 3.2% more EV charging in this scenario than in the reference scenario in 2035. By 2035, food-based diesel substitutes reach nearly 7 billion GGE, while waste oil-derived diesel substitutes increase to nearly 2.7 billion GGE; together, this marks an increase of 237% and 192% relative to 2020 consumption levels, respectively.

Scenario 2, illustrated in Figure 3b, represents the impact of a medium CI reduction of 20% by 2035 on the transport fuel mix. In this scenario, food-based renewable diesel increases significantly to nearly 19 billion GGE, while waste oil-derived diesel fuels increase to nearly 5.5 billion GGE. To meet the higher target level, corn ethanol production phases out towards 2030 to facilitate the greater blending of cellulosic ethanol with a lower CI score. The higher target level also increases the value of electric vehicle charging, resulting in an increase of electric charging of 7.6% by 2035 relative to the reference case.

Scenario 3, illustrated in Figure 3c, presents the impact of a 27% reduction in transport fuel CI by 2035, the largest CI reduction of any scenario in this analysis. This scenario, along with Scenario 6, generates the largest increase in alternative fuels of all the scenarios assessed, with total alternative fuel consumption approaching 62 billion GGE by 2035. The largest increase in blending occurs from soy-based and waste oil-based renewable diesel; together, these pathways reach approximately 35 billion GGE and 7 billion GGE, respectively. Cellulosic ethanol production increases significantly in this scenario, reaching the E10 blend wall by 2035 with approximately 8 billion GGE of production. This scenario also results in a total increase in EV charging of approximately 14% relative to the reference scenario.

The results from all three scenarios suggest a strong relationship between the GHG reduction target and the total quantity of food-based biofuels supplied to the market. Due to the blending constraint for ethanol, the majority of biofuel expansion in all three scenarios occurs in the smaller diesel fuel pool because renewable diesel can be blended into diesel without limits, despite the majority of deficits coming from the production of fossil gasoline. Figure 11 below illustrates the quantity of food-based biofuels, waste oil-derived biofuels, and second-generation fuels on the market across all scenarios in this analysis.

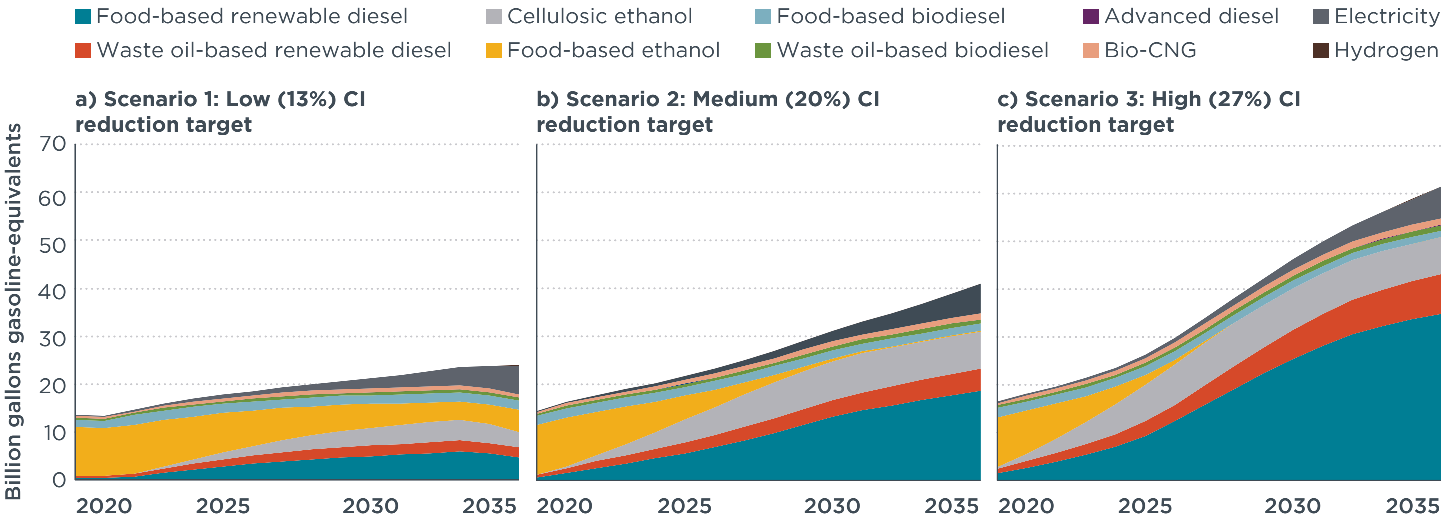

Figure 3. Mix of fuels supplied to the U.S. transport sector 2020–2035 in Scenario 1 with low (13%) CI reduction target, Scenario 2 with medium (20%) CI reduction target, and Scenario 3 with high (27%) CI reduction target

COMPARING THE IMPACT OF DIFFERENT ILUC FACTORS

The mix of fuels deployed in Scenario 4 is identical to that in Scenario 3 shown above in Figure 3c. The difference in GHG impacts between the two scenarios is due to the post-hoc ILUC analysis (the implications of that change is assessed in the discussion section below). Overall, this post-hoc ILUC emissions in this scenario increase the average carbon intensity of the transport fuel mix by approximately 10 gCO_2e/MJ in 2030—reducing the intended GHG savings from the policy by over a third of the intended 27% carbon intensity reduction.

Figure 4a illustrates the impact of incorporating higher ILUC factors in LCFS accounting for corn and soy-derived biofuels in Scenario 5; this results in a transition away from these fuels towards 2035. Because emissions from both fuel pathways exceed the fossil fuel baseline in this scenario, they initially generate deficits under the program and their contribution scales back quickly from current consumption levels. Unlike Scenarios 1 through 3, the food-based renewable diesel industry does not expand. In this scenario, like Scenarios 2 and 3, corn ethanol production declines in favor of cellulosic ethanol production up to the E10 blend wall. However, the majority of the new fuel production in this scenario comes from waste oil-derived renewable diesel, which expands to approximately 10.5 billion GGE. Electric vehicle charging increases by 8.7% in 2035 relative to the reference case.

The mix of fuels in Scenario 6, shown in Figure 4b below, illustrates a high GHG reduction target scenario using California LCFS ILUC values in place of EPA RFS ILUC values. The deployment of fuels here closely matches that of Scenario 3, primarily due to the similarities between CARB's ILUC values and EPA's ILUC assessment; however, we note that CARB estimates approximately 1/3 lower ILUC emissions for corn ethanol and 10% lower for soy biodiesel. Consequently, the share of food-based renewable diesel and biodiesel (nearly 40 billion GGE) is about 9% higher than in Scenario 3. Likewise, while maintaining the same credit price target of $650 per tonne, the overall target level increases slightly to a 28.4% CI reduction. This scenario also has slightly higher EV charging than in scenario 3, with charging increasing 15% in 2035 relative to the reference case.

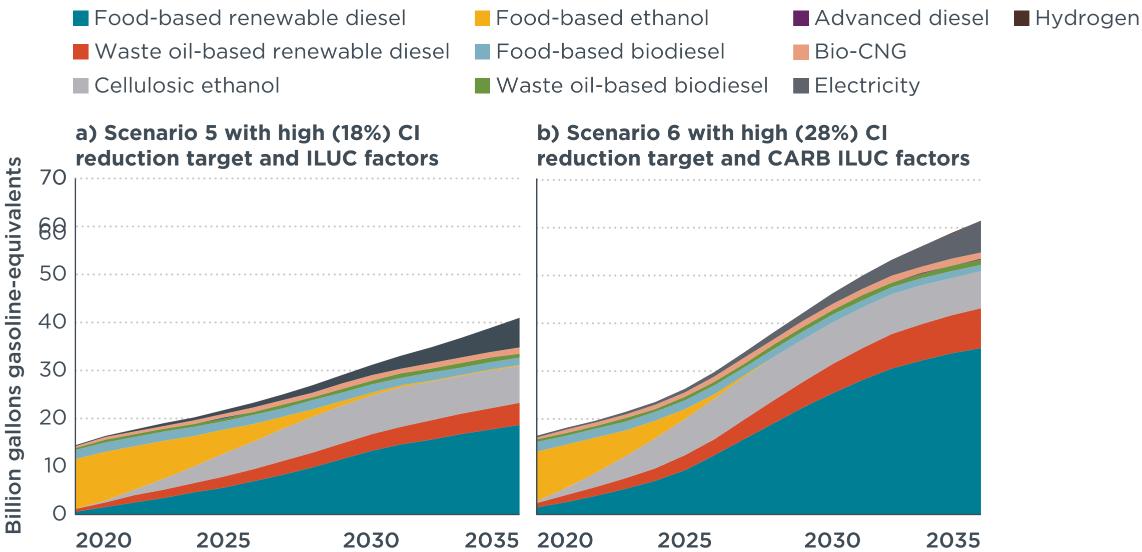

Figure 4. Mix of fuels supplied to the U.S. transport sector 2020–2035 in Scenario 6, high (28.4%) CI reduction target using CARB ILUC factors, and Scenario 6, high (28.4%) CI reduction target and CARB ILUC factors

COMPARING THE IMPACT OF FEEDSTOCK CAPS

Figure 5a illustrates the mix of fuels deployed over time in response to an LCFS with a high credit price ($650 per tonne) but paired with separate caps on the contribution of food-based biofuels and waste oil-derived biofuels in Scenario 7. The caps, set at 12.1 billion GGE for food-based biofuels and 0.9 billion GGE for waste oils, maintain these feedstocks' contribution at 2020 levels on an energy basis. Due in part to the greater expense posed by capping the contribution of these cheaper feedstocks, the targeted average fuel CI reduction for this scenario is 16.7% by 2035 to align with the intended credit price. The fuel deployment trajectory in this scenario differs substantially from Scenarios 1 through 3; notably, the contribution of food-based renewable diesel only increases to approximately 10 billion GGE. Here the food cap generates a transition from corn ethanol to cellulosic ethanol; by 2035, the food cap largely is met through soy-based renewable diesel, which has no blending constraints. Waste oil-based fuel consumption remains at 2020 levels throughout the time series. Notably, this pathway has the largest contribution of second-generation diesel fuels produced from lignocellulosic wastes and residues, which increase to 300 million GGE of production by 2035. In addition, EV charging increases by 7.8% relative to the reference case by 2035 in this scenario.

Figure 5b illustrates the mix of fuels supplied over time in Scenario 8, which incorporates a combined cap of 13 billion GGE for food-based biofuels and waste oil-derived biofuels. Here, the energy-based cap for food-based biofuels and waste oil derived biofuels is combined into one value, which can be met through the most cost-effective combination of fuels. This constraint reduces the contribution of the cheapest fuels to the overall CI target compared to scenario 3, and thus the target declines to a 18% CI reduction by 2035 to align with the $650 per tonne credit price target. In this scenario, total food-based biofuel production declines significantly to approximately

7 billion GGE, primarily due to the better cost-performance of waste oil-derived biofuels for generating LCFS credits. Consequently, waste oils provide the majority of fuels within the combined cap, increasing to approximately 6 billion GGE—a 540% increase relative to 2020 consumption. Together, cellulosic ethanol and advanced diesel increase to approximately 8 billion GGE in this scenario. Electric vehicle charging increases 8.6% by 2035 relative to the reference scenario.

Figure 5c shows the impact of a food-based biofuel-only cap on the mix of transport fuels supplied in 2020–2035, as described in Scenario 9. The contribution of food-based biofuels is limited to their 2020 consumption level of approximately 12.1 billion GGE. The target level is higher than the other safeguard scenarios, as waste oils have no restrictions on their contribution; therefore, the CI reduction target is 21.3% in 2035. In this scenario, renewable diesel production from waste oils increases significantly, exceeding 10 billion GGE by 2035. Due to the food-based biofuel cap, corn ethanol production phases out in favor of cellulosic ethanol production, and the food cap is primarily met through the increased production of soy-based renewable diesel, which increases to approximately 11 billion GGE by 2035, occupying the bulk of the food-based biofuel cap under this scenario. This scenario has the strongest EV charging response, as EV charging increases 10.5% by 2035 relative to the reference case.

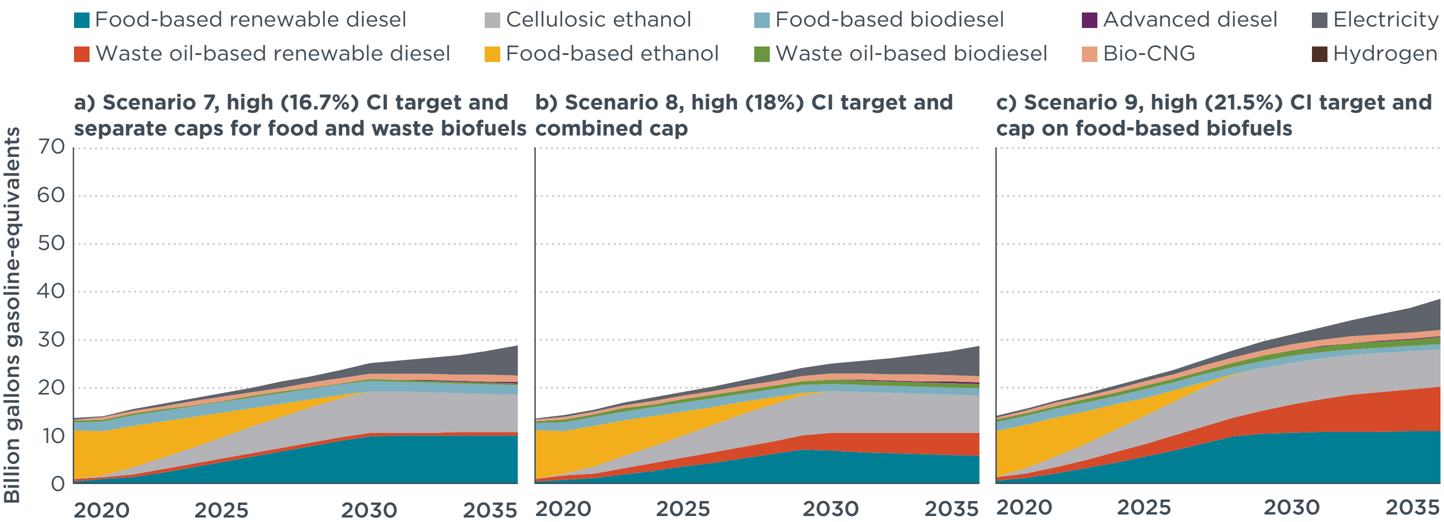

Figure 5. Mix of fuels supplied to the U.S. transport sector 2020–2035 in Scenario 7, high (16.7%) CI reduction target with separate caps for food and waste oil-derived biofuels, Scenario 8, high (18.0%) CI reduction target with a combined cap for food and waste oil biofuel, and Scenario 9, high (21.5%) CI reduction target with a cap on food-based biofuels

DISCUSSION

Across the full set of scenarios assessed, we find that a national-level LCFS without any feedstock-specific caps will greatly increase the demand for both food-based biofuels and waste oils. Figure 6 illustrates the total volume of fuels consumed in both categories in 2035, as well as the percentage change in consumption relative to 2020 levels. As shown, the estimated annual total contribution of ILUC emissions to the average on-road transport mix in 2035 for each scenario ranges from approximately 6 million to 330 million tonnes CO_2e. As a point of comparison to the volumes of food-based biofuels and waste oils depicted in Figure 11, the total second-generation and zero-emission fuel consumed in 2035 is relatively consistent across all scenarios with a $650 per tonne credit price, ranging from 7.8 billion to 8.2 billion GGE in Scenarios 2 through 9.

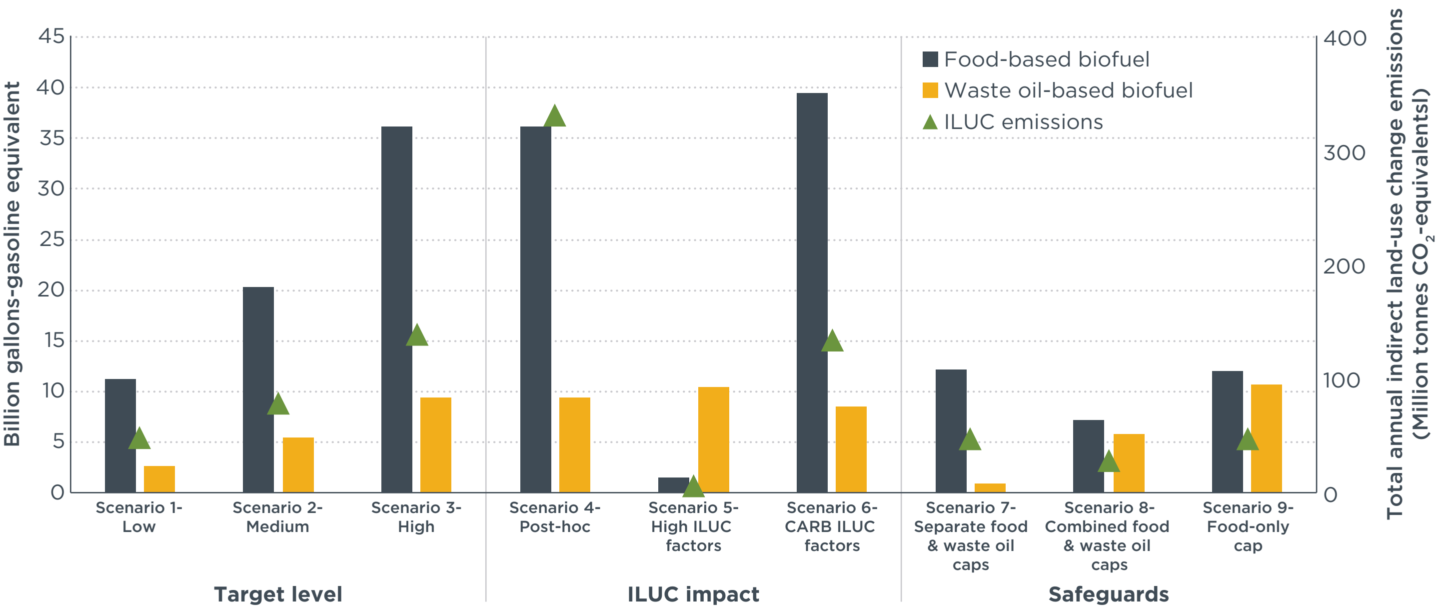

Figure 6. Projected 2035 volumes of food-based biofuels and waste oil-based biofuels presented alongside total ILUC emissions, across multiple LCFS implementation scenarios

In scenarios without any policy safeguards and using existing ILUC values for biofuels (Scenarios 1 through 3), we find that the overall LCFS target level is strongly correlated with food-based biofuel consumption. We find that an LCFS would maintain existing food-based biofuel consumption at the "low" GHG reduction target of 13%, whereas it would increase food-based biofuel consumption by 67% and nearly 200% in the medium and high GHG target scenarios, respectively. These three scenarios also show a substantial increase in waste oil consumption from animal fats and UCO, with consumption increasing by over 200% to 935% in these three scenarios to a volume of 2.7 billion to 9.4 billion GGE.

The quantity of waste oils used to comply with the LCFS by 2035 greatly exceeds the domestic resource base in all but one scenario, dwarfing the potential scale of genuine used cooking oil collection in Asia that could be used for imports. High demand for waste oils may induce fraud from virgin palm oil falsely claimed to be used cooking oil. The ILUC emissions from this palm oil may undermine a portion of the LCFS's intended emissions savings. Figure 7 illustrates the impact of waste oil imports on the average carbon intensity of the on-road fuels mix across different scenarios, as well as the quantity of waste oil imports in each scenario. We find that waste oil fraud emissions are highest when there is a high target level and no waste oil caps in place. We estimate that the ILUC impact from fraudulent palm oil alone can add up to 3.5 gCO_2e/MJ to the average on-road fuel carbon intensity.

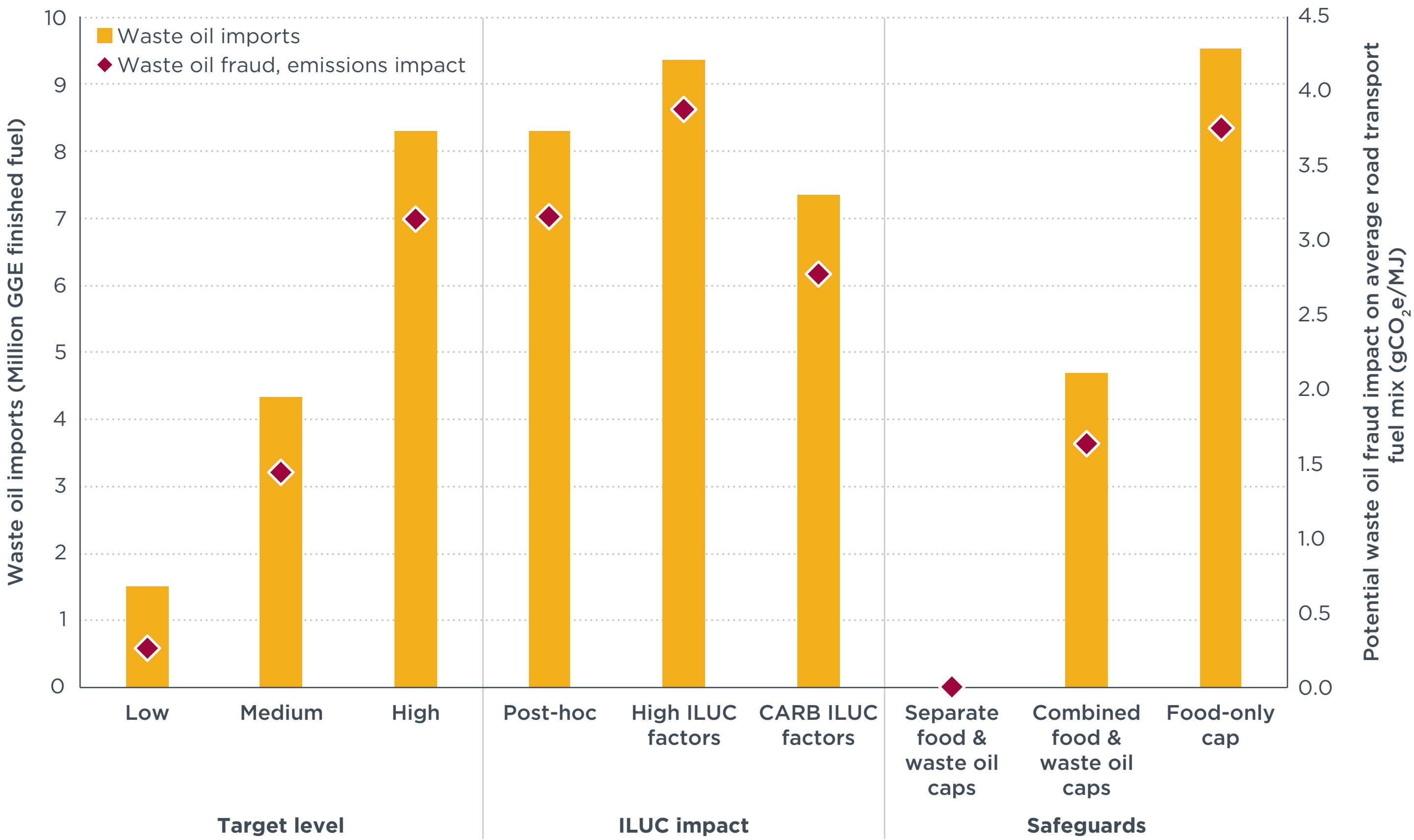

Figure 7. Quantity of LCFS-induced waste oil imports and GHG impact of waste oil fraud, across multiple LCFS implementation scenarios

In Scenarios 2 and 3, we illustrate that a medium or high GHG reduction target would drive increased food-based biofuel consumption; food-based biofuels would continue to contribute the bulk of the compliance under an LCFS for the timeline studied. However, the continued reliance on food-based biofuels may pose a risk if policymakers underestimate ILUC emissions and over-credit these fuels' GHG savings. To illustrate this risk in the *post-hoc* emissions Scenario (Scenario 4), we first estimate the mix of fuels used to reach compliance using the same target levels and emission factors used in Scenario 3, and then estimate what the true GHG emissions would be if ILUC emissions were higher than the regulatory values used. This impact is shown in Figure 8. We find that higher ILUC from corn and soy alone can increase the average CI of the on-road fuel mix by approximately 10 gCO_2e/MJ by 2035, erasing approximately half of the emissions savings from the policy.[8] This result is primarily attributable to the contribution of ILUC from soy, as in this scenario corn ethanol consumption declines in favor of cellulosic ethanol as soy-based renewable diesel consumption continues to increase. Incorporating high ILUC factors directly into the regulation, as implemented

8 Waste oil fraud could reduce the intended emissions savings by an additional 3 gCO_2e/MJ in 2035

in the High ILUC factors scenario (Scenario 5), would greatly decrease the incentive for food-based biofuel blending and the contribution of these fuels would decline precipitously (as shown in Figure 11). However, the lack of safeguards for waste oil imports in that scenario would increase the incentive for these feedstocks even further, resulting in the highest usage of waste oils in any scenario. The CARB ILUC factors scenario (Scenario 6), which uses lower ILUC factors for corn and soy than the first three scenarios, illustrates a slight increase in food-based biofuel consumption relative to the High Target Level Scenario (Scenario 3).

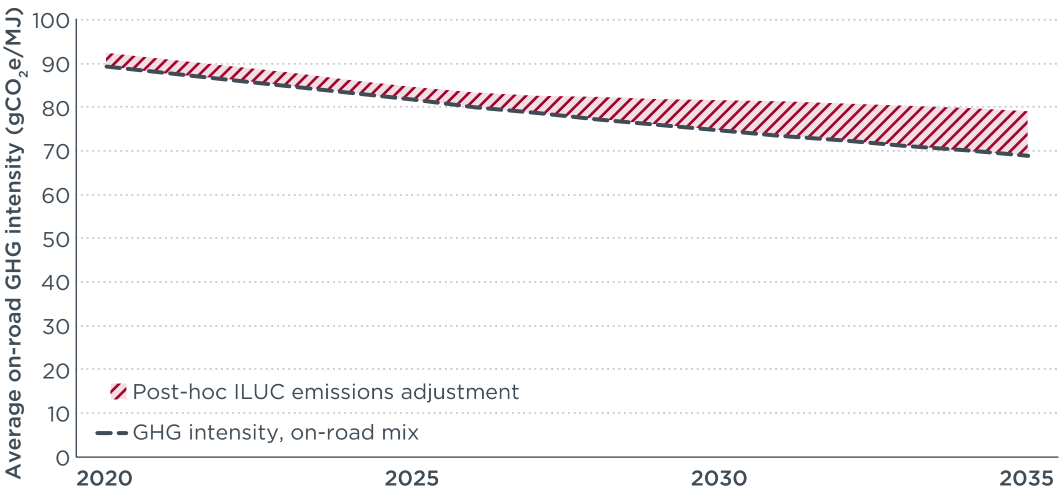

Figure 8. Average on-road GHG intensity for high target level LCFS scenario with the impact of additional, post-hoc ILUC emissions

Next, we evaluate several safeguards that could be implemented to protect against unintended indirect emissions and safeguard the efficacy of an LCFS program. The final set of three scenarios evaluates the impact of including explicit, energy-based caps on the consumption of first-generation food-based biofuels and waste-oil derived biofuels. We find that a cap on the contribution from food-based biofuels at 2020 consumption levels in Scenario 9 would prevent an increase food-based biofuel consumption but would drive a large increase in waste oils biofuel. A combined cap, as illustrated in Scenario 8, would reduce food-based biofuel consumption in favor of greater waste oil use. While the quantity of waste oils used in Scenario 8 is lower here than in most scenarios, it still exceeds 4 billion GGE and poses a high risk of fraud. Therefore, we find that only with separate caps for the contributions of food-based and waste oil-based biofuels, as in Scenario 7, would the risks by these pathways be effectively managed. There would be no additional waste oil fraud emissions in Scenario 7, while the food-based biofuel consumption is capped at 2020 levels.

Overall, we find that in most scenarios, the role of second-generation biofuels is constrained by the relative cost-effectiveness of credit generation by food-based and waste oil-derived biofuels. In most cases, the higher emissions from food-based biofuels are offset by their lower production costs, and thus offer lower-cost compliance compared to second-generation biofuels. The highest uptake of second-generation and zero-carbon fuels occurs when there are high credit prices and caps constraining the use of first-generation biofuels. Across the scenarios assessed, we estimate that cellulosic ethanol produced from agricultural residues and energy crops is incentivized at medium and high credit price levels of $450 and $650 per tonne, respectively. In these scenarios, cellulosic ethanol begins to displace conventional corn ethanol starting in 2025, largely due to the relatively high emissions of conventional corn ethanol and the lower price of cellulosic ethanol compared to second-generation diesel pathways. However, the overall deployment of cellulosic ethanol is largely constrained by the E10 blend wall. Deployment of second-generation diesel pathways, including cellulosic drop-in diesels and electrofuels, is extremely low in most scenarios. Its highest deployment occurs in Scenario 7, largely due to constraints imposed by the cap on food-based and waste oil-based biofuels; here, cellulosic drop-in diesel production increases to 300 million GGE by 2035.

We find that a national LCFS could accelerate EV deployment by 3%–15%. In our analysis, a substantial portion of the LCFS targets in 2035 is met by the increased deployment of electric vehicles, and most of this increase would occur anyway because of complementary policies. Electric vehicle charging displaces approximately 19 billion GGE of gasoline demand in 2035, after factoring in the energy efficiency ratio of EV's. We find that total EV miles driven are higher in each of the National LCFS scenarios compared to the reference scenario. Across the scenarios, we estimate that EV charging generates from 36% to 59% of the credits necessary to achieve compliance in 2035—in excess of 120 million credits by 2035 and a higher contributor than any liquid fuel pathway. We estimate that there will be some degree of additional EV deployment attributable to the credit values generated by charging and re-invested via reduced charging costs and rebates; the change in electricity supplied to the transport sector would range from 3.2% to 15.0% relative to the reference case in 2035, as illustrated in Figure 9. We find that in general, EV deployment would respond to higher credit prices and higher target levels, though this response is much smaller than the ongoing year-over-year growth driven by ZEV standards in the reference case.

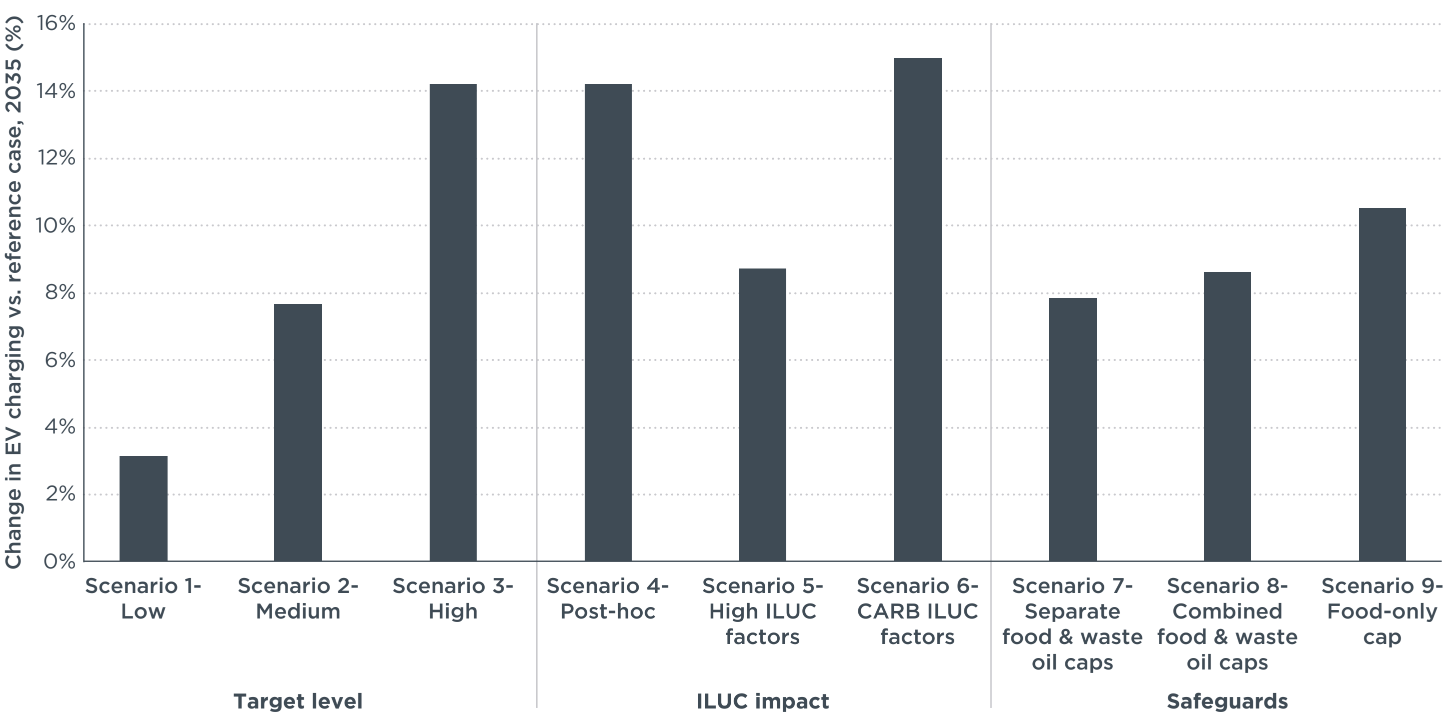

Figure 9. Change in electric vehicle charging in 2035 for each scenario, compared to the reference case

Several important compliance options fall outside the scope of this analysis, particularly CI reductions through further facility improvements and the use of higher ethanol blends. A key component of the LCFS program structure is to incentivize greater fuel production efficiency, so that fuel producers have an incentive to improve the CI of their fuels. Fuel production facilities have likely already made such improvements and it is unknown what potential there is for further improvements. Though we include a pathway for corn ethanol with carbon capture and sequestration, we did not model any other potential improvements. We may thus potentially underestimate the potential for facility improvements to contribute to the GHG targets. We also note that our assumption of a binding E10 blend wall greatly impacted this analysis, with the bulk of compliance in the liquid fuel pool coming from drop-in diesel substitutes. With a higher cap on ethanol consumption and greater availability of E85 vehicles, there would be potential for greater cellulosic ethanol consumption and thus greater compliance in the gasoline fuel pool.

CONCLUSION

Uncertainty over the future of the U.S. Renewable Fuel Standard and a desire to deploy greater volumes of second-generation fuels have prompted interest among policymakers for a national LCFS based on similar policies in states like California. Advocates for a national LCFS argue that a GHG intensity target for the transport fuel sector, along with carbon pricing, will drive the production of new fuels, improve the effectiveness of existing fuel pathways, and reduce overall transport emissions to a greater degree than the current volumetric RFS. However, we find that if a fully technology-neutral national LCFS is implemented, it may largely incentivize greater volumes of existing, commercialized fuel pathways and fail to induce the deployment of appreciable volumes of second-generation biofuels.

We find that a fully technology-neutral national LCFS would greatly increase demand for food-based biofuels. We estimate that the contribution of food-based biofuels would increase up to up to 220% relative to 2020 levels with a high target level in place. Though we include ILUC emission factors for food-based biofuels such as soy, these feedstocks still contribute the bulk of biofuel compliance in most scenarios—particularly soy renewable diesel, which can be used without any blending constraints. Overall, we find that it is cheaper to blend these fuels in higher quantities than to blend smaller quantities of more expensive second-generation fuels with lower CI scores. Furthermore, we find that LCFS compliance is highly sensitive to ILUC factors—using the lower ILUC factors in Scenario 6 increases the consumption of food-based biofuels in 2035 by 9% relative to the high target Scenario 3, whereas using higher ILUC factors results in a steep decrease in food-based biofuel of nearly 100% in scenario 5.

This analysis finds that the choice of ILUC factors assigned to fuel pathways not only influences the mix of fuels used to meet the policy targets but may also influence the integrity of the policy. The effectiveness of an LCFS is determined largely by the quality of its underlying carbon accounting. If ILUC is underestimated, for example, it could systematically undermine the intended GHG savings from the policy. We find that by using a post-hoc adjustment for ILUC emissions to assign a higher ILUC value than EPA's current set of estimates, the emissions savings from the LCFS would be nearly halved in the high target scenario, and the *de-facto* on-road average transport fuel emission would be approximately 10.1 gCO_2e/MJ higher.

This study estimates that a national LCFS may increase demand for waste oils in excess of the domestic supply and may incentivize imported waste oils with sustainability risks. Waste oils such as used cooking oil may be converted into drop-in biofuels with low-carbon intensities that have high policy value and relatively low production costs. However, true waste oils are a highly constrained resource that are largely already utilized domestically. We estimate that without safeguards, waste oil biofuel volumes would increase by as much as ten times. This quantity cannot plausibly be supplied by genuine waste oil collection in Asia, and risks being supplied through fraudulently labeled virgin vegetable oil. We find that waste oil fraud could increase the average on-road carbon intensity of transport fuels by up to 4 gCO_2e/MJ in some scenarios and undermine a portion of the GHG savings from the policy.

We find that feedstock-specific caps could limit indirect emissions risks and improve the integrity of an LCFS. Energy-based caps on the contribution of the riskiest feedstocks, such as food-based biofuels and waste oil-derived fuels, could greatly mitigate the impact of ILUC emissions and waste oil fraud on the effectiveness of the policy. Though the scenario with these safeguards is more challenging to meet, it has much higher integrity of its targets, with similar GHG savings, even when post-hoc ILUC adjustments and waste oil fraud impacts are included in the average estimated on-road carbon intensity. Capping the contribution of riskier, first-generation pathways also creates a stronger signal for second-generation cellulosic fuels—the production of these fuels increases by 300 million GGE relative to the high target scenario. However, we find that in the absence of separate caps for waste oils and food-based biofuels, it is likely that the waste oil use could grow substantially even as food-based biofuel declines. Without these specific safeguards, we find a high risk that a national LCFS would not deliver the level of GHG reductions necessary nor advance the production of second-generation biofuels industry sufficiently to promote the deep decarbonization of the U.S. transport sector.

Overall, we find that the transition to a national LCFS from the present-day volumetric RFS presents several clear risks, particularly by expanding the use of food-based biofuels and waste oil-derived biofuels, without necessarily providing a similar incentive for second-generation biofuels. However, we find that many of these risks can be addressed by changing the technology-neutral structure of the LCFS and implementing caps on the contributions from the riskiest pathways. We find that this approach could help to build on the structural improvements of a carbon intensity standard, ensure the integrity of its carbon savings, and provide a stronger signal for second-generation biofuels with high GHG savings.

REFERENCES

Brown, A., Waldheim, L., Landalv, I., Saddler, J., Ebadian, M., Mcmillan, J. D., Bonomi, A., & Klein, B. (n.d.). *Advanced Biofuels – Potential for Cost Reduction* (p. 88). IEA Bioenergy. https://www.ieabioenergy.com/wp-content/uploads/2020/02/T41_CostReductionBiofuels-11_02_19-final.pdf.

Bushnell, J., Mazzone, D., Smith, A., & Witcover, J. (2020). *Uncertainty, Innovation, and Infrastructure Credits: Outlook for the Low Carbon Fuel Standard Through 2030*. https://doi.org/10.7922/G2XD0ZXH.

California Air Resources Board (CARB). (2015). *Detailed analysis for indirect land use change*. https://ww2.arb.ca.gov/sites/default/files/classic/fuels/lcfs/iluc_assessment/iluc_analysis.pdf.

California Air Resources Board (CARB). (2021). *LCFS Data Dashboard*. https://ww3.arb.ca.gov/fuels/lcfs/dashboard/dashboard.htm.

California Low Carbon Fuel Standard Regulation, CCR 17 sections 95480 (2020). https://ww2.arb.ca.gov/sites/default/files/2020-07/2020_lcfs_fro_oal-approved_unofficial_06302020.pdf.

Corey, R., Buffington, M., & Hatton, L. (2011). *Low Carbon Fuel Standard 2011 Program Review Report*. California Air Resources Board (CARB).

Court of Rotterdam. (2020). *Kort geding, opheffing conservatoir beslag op inhoud 39 containers biobrandstof tegen zekerheidsstelling. ECLI: NL: RBROT: 2020: 11063*. https://uitspraken.rechtspraak.nl/inziendocument?id=ECLI:NL:RBROT:2020:11063.

Daniel Mazzone, J. W. (2021). *Multijurisdictional Status Review of Low Carbon Fuel Standards, 2010–2020 Q2: California, Oregon, and British Columbia*. https://doi.org/10.7922/G2SN0771.

Directive 2009/30/EC of the European Parliament and of the Council of 23 April 2009 amending Directive 98/70/EC as regards the specification of petrol, diesel and gas-oil and introducing a mechanism to monitor and reduce greenhouse gas emissions and amending Council Directive 1999/32/EC as regards the specification of fuel used by inland waterway vessels and repealing Directive 93/12/EEC (Text with EEA relevance, Pub. L. No. Directive 2009/30/EC, OJ L 140, 5.6.2009 88 (2009).

Energy Information Administration (EIA). (2020a). *Annual Energy Outlook 2020*. https://www.eia.gov/outlooks/archive/aeo20/.

Energy Information Administration (EIA). (2020b). *Petroleum Marketing Monthly (PMM)*. https://www.eia.gov/petroleum/marketing/monthly/.

European Anti-Fraud Office. (2019). *The OLAF Report*. https://ec.europa.eu/anti-fraud/system/files/2021-09/olaf_report_2019_en.pdf.

Ferris, M. C., Dirkse, S. P., Jagla, J.-H., & Meeraus, A. (2009). An extended mathematical programming framework. *Computers & Chemical Engineering*, *33*(12), 1973–1982. https://doi.org/10.1016/j.compchemeng.2009.06.013

Food and Agriculture Organization (FAO). (n.d.). *FAOSTAT: Vegetable oil projections: Consumption, food*. Retrieved October 8, 2021, from http://www.fao.org/faostat/en/.

Food Safety and Standards Authority of India. (n.d.). *Background Note on Used Cooking Oil*. https://fssai.gov.in/ruco/background-note.php.

Canada Gazette, Part 1, Volume 154, Number 51, (2020). https://gazette.gc.ca/rp-pr/p1/2020/2020-12-19/html/reg2-eng.html.

GreenEA. (2021, January 6). *The Year 2021: Which Investments Will See the Light in the Biofuel Industry?* https://www.greenea.com/wp-content/uploads/2021/01/Greenea-Horizon-2030-Which-investments-will-see-the-light-in-the-biofuel-industry-1.pdf.

Greenhouse Gas Reduction (Renewable and Low Carbon Fuel Requirements) Act: Renewable and Low Carbon Fuel Requirements Regulation, Pub. L. No. O.C. 907/2008, B.C. Reg. 394/2008. https://www.bclaws.gov.bc.ca/civix/document/id/complete/statreg/394_2008.

Guest, G., & Desjardins, R. (2017). Impact of uncertainty in indirect land-use changes and life-cycle carbon intensity for biofuels under climate legislation: A case study of British Columbia. *Biofuels*, *8*(5), 605–613. https://doi.org/10.1080/17597269.2016.1242691.

House Select Committee on the Climate Crisis. (2020). *Solving the Climate Crisis: The Congressional Action Plan for a Clean Energy Economy and a Healthy, Resilient, and Just America* [Majority Staff Report]. U.S. Congress. https://climatecrisis.house.gov/sites/climatecrisis.house.gov/files/Climate%20Crisis%20Action%20Plan.pdf.

International Civil Aviation Organization (ICAO). (2019). *CORSIA Eligible Fuels – Life Cycle Assessment Methodology* [CORSIA Supporting Document]. https://www.icao.int/environmental-protection/CORSIA/Documents/CORSIA%20Supporting%20Document_CORSIA%20Eligible%20Fuels_LCA%20Methodology.pdf.

Kelly, S., & Renshaw, J. (2020, November 20). Exclusive: Plotting future, U.S. biofuel industry seeks federal clean fuel program from Biden. *Reuters*. https://www.reuters.com/article/us-usa-biofuels-carbon-exclusive-idUSKBN28100O.

Kharina, A., Searle, S., Rachmadini, D., & Prionggo, A. (2018). *Potential economic, health, and greenhouse gas benefits of incorporating used cooking oil into Indonesia's biodiesel*. Retrieved form the International Council on Clean Transportation https://theicct.org/publications/uco-biofuel-benefits-indonesia.

Lei Ordinária 13.576, de 26.12.2017.

Lutsey, N. (2015). *Global climate change mitigation potential from a transition to electric vehicles*. Retrieved from the International Council on Clean Transportation https://theicct.org/publication/global-climate-change-mitigation-potential-from-a-transition-to-electric-vehicles/.

Lutsey, N., & Nicholas, M. (2019). *Update on electric vehicle costs in the United States t hrough 2030*. Retrieved from the International Council on Clean Transportation https://theicct.org/publications/update-US-2030-electric-vehicle-cost.

Moultak, M., Lutsey, N., & Hall, D. (2017). *Transitioning to zero-emission heavy-duty freight vehicles*. Retrieved from the International Council on Clean Transportation https://theicct.org/publications/transitioning-zero-emission-heavy-duty-freight-vehicles.

Nicholas, M. (2019). *Estimating electric vehicle charging infrastructure costs across major U.S. metropolitan areas*. Retrieved from the International Council on Clean Transportation https://theicct.org/publications/charging-cost-US.

Oregon Department of Environmental Quality. (2021). *Oregon Clean Fuels Program Overview*. https://www.oregon.gov/deq/ghgp/cfp/Pages/CFP-Overview.aspx.

Pavlenko, N., Searle, S., & Christensen, A. (2019). *The cost of supporting alternative jet fuels in the European Union.* Retrieved from the International Council on Clean Transportation https://theicct.org/sites/default/files/publications/Alternative_jet_fuels_cost_EU_2020_06_v3.pdf.

Plevin, R. J., Beckman, J., Golub, A. A., Witcover, J., & O'Hare, M. (2015). Carbon Accounting and Economic Model Uncertainty of Emissions from Biofuels-Induced Land Use Change. *Environmental Science & Technology*, *49*(5), 2656–2664. https://doi.org/10.1021/es505481d.

Plevin, R. J., Delucchi, M. A., & O'Hare, M. (2017). Fuel carbon intensity standards may not mitigate climate change. *Energy Policy*, *105*, 93–97. https://doi.org/10.1016/j.enpol.2017.02.037.

Reducing greenhouse gas emissions by reducing the carbon intensity of transportation fuel., no. HB 1091-2021-22, Washington State Legislature (2021). https://app.leg.wa.gov/billsummary?BillNumber=1091&Initiative=false&Year=2021

Renewable and Low Carbon Fuel Requirements Regulation, B.C. Reg. 394/2008 O.C. 907/2008. Retrieved October 6, 2021, from https://www.bclaws.gov.bc.ca/civix/document/id/complete/statreg/394_2008.

Schmidt, P., Weindorf, W., Roth, A., Batteiger, V., & Riegel, F. (2016). *Power-to-Liquids – Potentials and Perspectives for the Future Supply of Renewable Aviation Fuel*. Retrieved from Umweltbundesamt. https://www.umweltbundesamt.de/en/publikationen/power-to-liquids-potentials-perspectives-for-the.

Spath, P. L., & Mann, M. K. (2004). *Life Cycle Assessment of Renewable Hydrogen Production via Wind/Electrolysis: Milestone Completion Report*. https://www.nrel.gov/docs/fy04osti/35404.pdf.

Sperling, D., Fulton, L., Arroyo, V., Aultman-Hall, L., Goetz, M., & Rubin, J. (n.d.). *5.2 Accelerating Deep Decarbonization in the U.S. Transportation Sector*. 25.

U.S. Department of Agriculture (USDA) Economic Research Service. (2020). *U.S. Bioenergy Statistics*. https://www.ers.usda.gov/data-products/us-bioenergy-statistics/.

U.S. Environmental Protection Agency (EPA). (n.d.). *Public Data for the Renewable Fuel Standard [Data and Tools].* https://www.epa.gov/fuels-registration-reporting-and-compliance-help/public-data-renewable-fuel-standard.

U.S. Environmental Protection Agency (EPA). (2010). *Renewable Fuel Standard: Final Regulatory Impact Analysis* (Regulatory Impact Analysis EPA-420-R-10-003). https://nepis.epa.gov/Exe/ZyPURL.cgi?Dockey=P1006DXP.txt.

U.S. Environmental Protection Agency (EPA). (2009). *EPA Lifecycle Analysis of Greenhouse Gas Emissions from Renewable Fuels*. https://nepis.epa.gov/Exe/ZyPDF.cgi?Dockey=P100B3F8.pdf.

van Grinsven, A., van den Toorn, E., van der Veen, R., & Kampman, B. (2020). *Used Cooking Oil (UCO) as biofuel feedstock in the EU*. CE Delft. https://www.transportenvironment.org/sites/te/files/publications/CE_Delft__200247_UCO_as_biofuel_feedstock_in_EU_FINAL%20-%20v5_0.pdf.

Wang, M., Elgowainy, A., Lee, U., Bafana, A., Benavides, P., Burnham, A., Cai, H., Dai, Q., Gracida, U., Hawkins, T., Jaquez, P., Kelly, J., Kwon, H., Liu, X., Lu, Z., Ou, L., Sun, P., Winjobi, O., Xu, H., … Zang, G.. (2020). *Greenhouse gases, Regulated Emissions, and Energy use in Technologies (GREET) Model ® (2020 Excel)*. Argonne National Laboratory (ANL), Argonne, IL (United States). https://doi.org/10.11578/GREET-EXCEL-2020/DC.20200912.1.

Witcover, J. (2018). *Status Review of California's Low Carbon Fuel Standard, 2011–2018 Q1 September 2018 Issue* [Research Report – UCD-ITS-RR-18-25]. UC Davis Institute of Transportation Studies. https://escholarship.org/uc/item/445815cd.

Witcover, J., & Murphy, C. (2021). Oregon's Clean Fuels Program: A Review and Status Update. *Transportation Research Record*, *2675*(3), 367–378. https://doi.org/10.1177/0361198120972394.

Wolinetz, M. (2014). *Biofuels in Canada 2020: Tracking biofuel consumption, feedstocks and avoided greenhouse gas emissions*. Retrieved from Navius Research https://www.naviusresearch.com/publications/renewable-low-carbon-fuel-requirement-regulation/.

Woltjer, G., Daioglou, V., Elbersen, B., Barberena Ibanez, G., Smeets, E., Sanchez Gonzalez, D., & Gil Barno, J. (2017). *Analysis of the latest available scientific research and evidence on indirect land use change (ILUC) greenhouse gas emissions associated with production biofuels bioliquids*. https://ec.europa.eu/energy/studies_main/final_studiesanalysis-latest-available-scientific-research-and-evidence-indirect-land_en.

Yeh, S., Sperling, D., Griffin, M., Khanna, M., Leiby, P., Msangi, S., Rhodes, J., & Rubin, J. (2012). National Low Carbon Fuel Standard: Policy Design Recommendations. *SSRN Electronic Journal*. https://doi.org/10.2139/ssrn.2105897.

Yeh, S., Witcover, J., Lade, G. E., & Sperling, D. (2016). A review of low carbon fuel policies: Principles, program status and future directions. *Energy Policy*, *97*, 220–234. https://doi.org/10.1016/j.enpol.2016.07.029.

Zhou, Y., Baldino, C., & Searle, S. (2020). *Potential biomass-based diesel production in the United States by 2032*. Retrieved from the International Council on Clean Transportation https://theicct.org/publications/potential-biomass-based-diesel-production-united-states-2032.

APPENDIX A: DATA INPUTS

Table A1. LCA and cost data inputs for fuel compliance modeling

Fuel pathway	Direct LCA emissions	Source	Cost ($/gal)	Source
Fossil gasoline	93.1	EPA (2010); RFS baseline value	2.12	EIA (2020b), Five-year average price via EIA Refiner Petroleum Product Prices by Sales Type
Fossil diesel	91.9	EPA (2010); RFS baseline value	1.90	EIA (2020b), Five-year average price via EIA Refiner Petroleum Product Prices by Sales Type
Soy biodiesel	30.3	Wang et al. (2020)	3.24	USDA ERS (2020), Based on five-year average of U.S. soy biodiesel prices
Canola biodiesel	29.8	Wang et al. (2020)	3.73	USDA (2020), Based on five-year average of U.S. soy biodiesel prices; adjusted for higher canola oil price
Used cooking oil biodiesel	20	CARB (2020); average LCFS-certified pathways in California	2.41	USDA (2020), Based on five-year average of U.S. soy biodiesel prices; adjusted for lower waste oil price
Tallow biodiesel	23	Wang et al. (2020)	2.41	USDA (2020), Based on five-year average of U.S. soy biodiesel prices; assume same price as UCO
White grease biodiesel	23	Assume same as tallow biodiesel	2.41	USDA (2020), Based on five-year average of U.S. soy biodiesel prices; assume same price as UCO
Fat biodiesel	23	Assume same as tallow biodiesel	2.41	USDA (2020), Based on five-year average of U.S. soy biodiesel prices; assume same price as UCO
Corn oil biodiesel	10.6	Wang et al. (2020)	3.24	USDA (2020), Based on five-year average of U.S. soy biodiesel prices; adjusted for corn oil price
Soy renewable diesel	21.6	Wang et al. (2020)	4.25	Pavlenko et al. (2019)
Canola renewable diesel	30.5	Wang et al. (2020)	4.81	Pavlenko et al. (2019); adjusted for higher feedstock price
Used cooking oil renewable diesel	20.1	CARB (2020); average LCFS-certified pathways in California	3.58	Pavlenko et al. (2019)
Tallow renewable diesel	21	Wang et al. (2020)	3.58	Pavlenko et al. (2019); assume same as UCO price
White grease renewable diesel	21	Assume same as tallow renewable diesel	3.58	Pavlenko et al. (2019); assume same as UCO price
Animal fat renewable diesel	21	Assume same as tallow renewable diesel	3.58	Pavlenko et al. (2019); assume same as UCO price
Corn oil renewable diesel	11	Wang et al. (2020)	4.40	Pavlenko et al. (2019); adjusted for higher feedstock price
Agricultural residue cellulosic diesel	7.7	Wang et al. (2020)	6.87	Pavlenko et al. (2019), diesel share
Forest residue cellulosic diesel	10.4	Wang et al. (2020)	7.21	Pavlenko et al. (2019), diesel share
MSW cellulosic diesel	15.0	CARB (2015b)	5.20	
Power-to-liquid diesel	1	Schmidt et al. (2016)	11.49	Searle and Christensen (2018); using $2.50/liter policy support as a midrange value
Green hydrogen, 2020	1.8	Spath and Mann (2004)	7.92	Christensen (2020); assume 33rd percentile of U.S. mid-price electricity forecast
Green hydrogen, 2035	1.8	Spath and Mann (2004)	6.19	Christensen (2020); assume 33rd percentile of U.S. mid-price electricity forecast

Fuel pathway	Direct LCA emissions	Source	Cost ($/gal)	Source
Grid electricity, 2020	106.1	EIA (2020)	0.17	Based on EIA end-use (retail) electricity price, factoring in charging infrastructure cost, demand charges & share of DCFC, Level 2 Public and residential charging as in Kelly and Pavlenko (2020)
Grid electricity, 2035	88.8	EIA (2020)	0.14	Based on EIA end-use (retail) electricity price, factoring in charging infrastructure cost, demand charges & share of DCFC, Level 2 Public and residential charging as in Kelly and Pavlenko (2020)
Bio-CNG	13.5	Wang et al. (2020), animal manure RNG	2.33	Pavlenko and Searle (2018), assuming mid price at $5 per GGE
Fossil CNG	74	EPA (2010); RFS baseline value	0.63	EIA (2020)
Agricultural residue cellulosic ethanol	8.3	Wang et al. (2020)	3.43	Brown et al. (2020); average of cellulosic ethanol range
Energy crop cellulosic ethanol	11.7	Wang et al. (2020)	3.43	Brown et al. (2020); average of cellulosic ethanol range
Agricultural residue cellulosic ethanol with CCS	-78.01	Wang et al. (2020); adjusted for 95% CO_2 capture	3.70	Brown et al. (2020); average of cellulosic ethanol range; assume $38/tonne carbon capture cost
Energy crop cellulosic ethanol with CCS	-74.41	Wang et al. (2020); adjusted for 95% CO_2 capture	3.70	Brown et al. (2020); average of cellulosic ethanol range; assume $38/tonne carbon capture cost
Corn ethanol	53.5	Wang et al. (2020)	1.60	USDA (2020), Based on five-year average of U.S. ethanol rack price
Corn ethanol with CCS	21.5	Wang et al. (2020); adjusted for 95% CO_2 capture	1.70	USDA (2020), Based on five-year average of U.S. ethanol rack price; assume $38/tonne carbon capture cost
Sugarcane ethanol	33.5	Wang et al. (2020)	2.52	Five-year average ethanol price at FOB, 61 cents per liter
Sorghum ethanol	56	Wang et al. (2020)	1.60	USDA (2020), Based on five-year average of U.S. ethanol rack price; same as corn ethanol price

Table A2. Vehicle data inputs for vehicle cycle modeling

Vehicle type	Fuel economy		Source	Cost		Source	Annual VMT
	2020	2035		2020	2035		
Gasoline LDV	28.3 mi/gal	34.1 mi/gal	Lutsey et al. (2019)	30,390	31,984	Lutsey et al. (2019)	11,500
Diesel HDV	7.5 mi/gal	10.8 mi/gal	ICCT Roadmap Tool	135,000	175,000	Moultak et al. (2017)	62,750
Electric LDV	3.4 mi/Kwh	3.7 mi/kWh	Lutsey et al. (2019)	40,000	23,209	Lutsey et al. (2019)	11,500
H2 HDV	8.5 mi/kg	9.8 mi/kg	Moultak et al. (2017)	226394	197,820	Moultak et al. (2017)	62,750
CNG HDV	6.0 mi/diesel-equivalent gallon	7.6 mi/diesel-equivalent gallon	Moultak et al. (2017)	202,216	197,820	Moultak et al. (2017)	62,750

APPENDIX B: SENSITIVITY ANALYSIS

The charts and figures in the main body of this report summarize the median results for each scenario. Here we present a series of histograms to illustrate the total range in results for both credit price and total GHG savings for each scenario. For Scenario 4, which includes a post-hoc ILUC assessment, we include both a histogram of the emissions reductions with and without the post-hoc ILUC emissions.

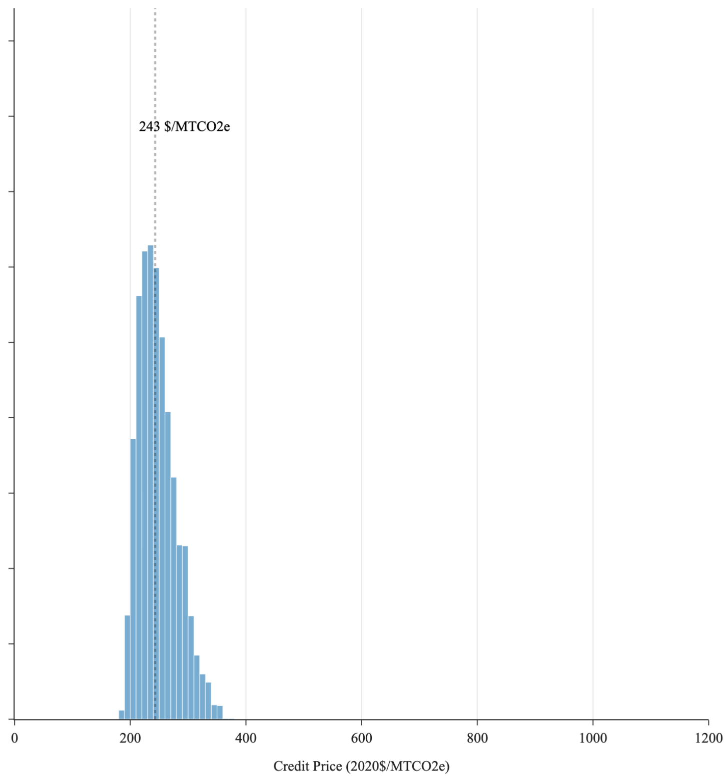

Figure B1. Distribution of 2035 LCFS credit prices across model runs, Scenario 1

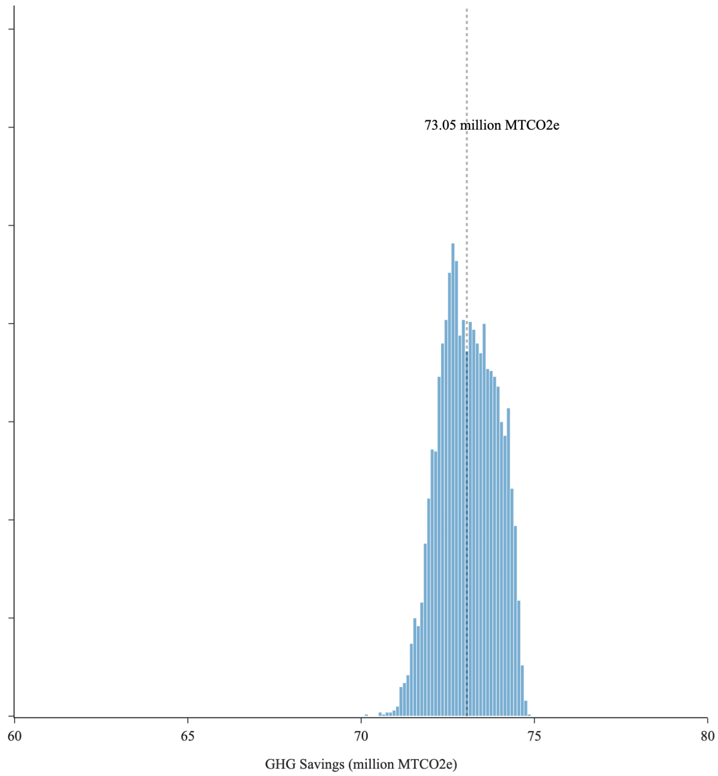

Figure B2. Distribution of 2035 total GHG reductions across model runs, Scenario 1

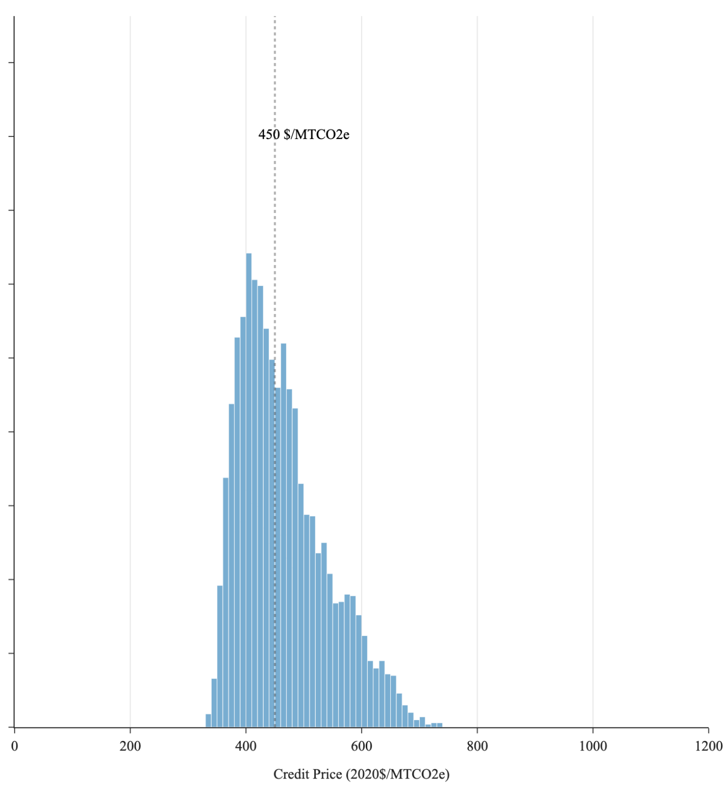

Figure B3. Distribution of 2035 LCFS credit prices across model runs, Scenario 2

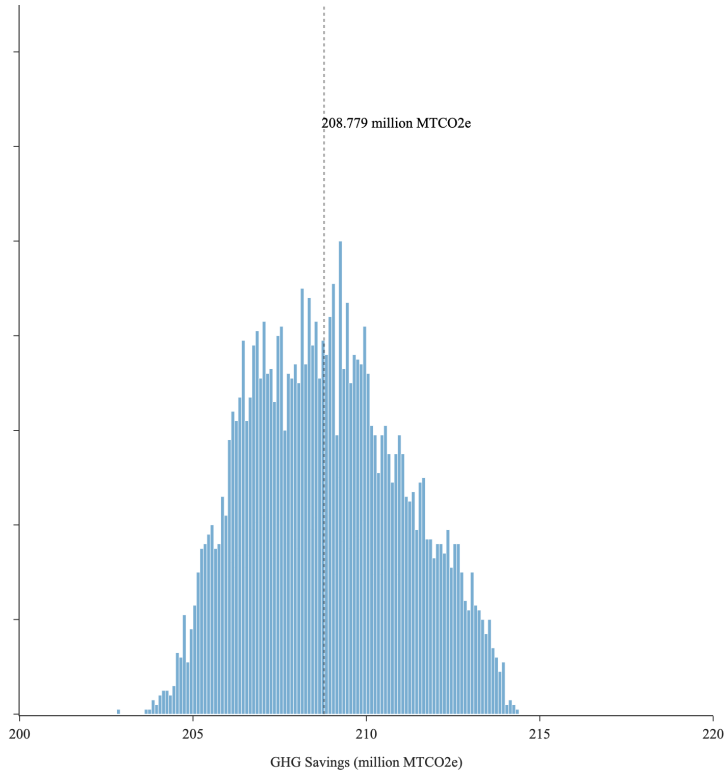

Figure B4. Distribution of 2035 total GHG reductions across model runs, Scenario 2

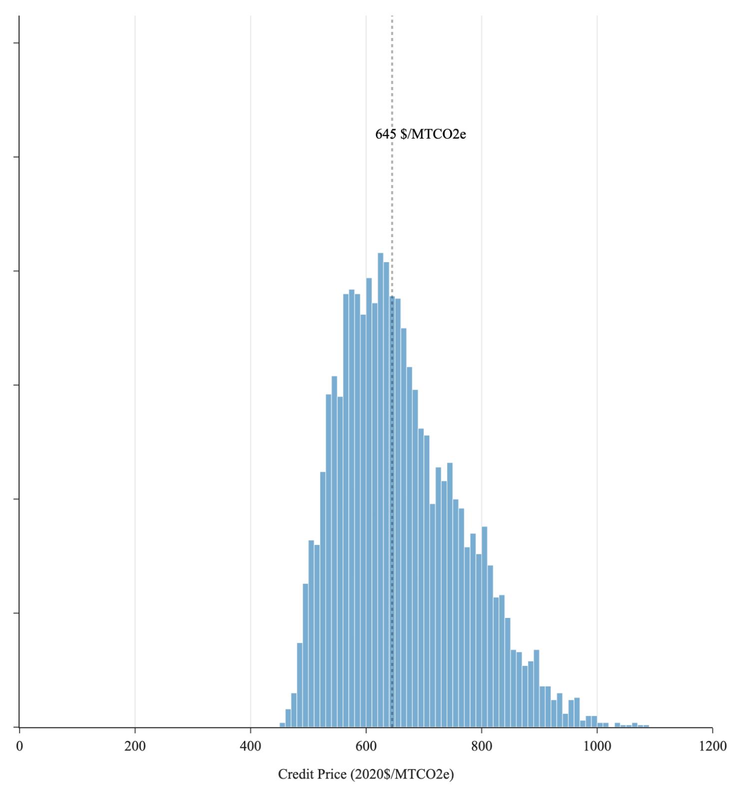

Figure B5. Distribution of 2035 LCFS credit prices across model runs, Scenario 3

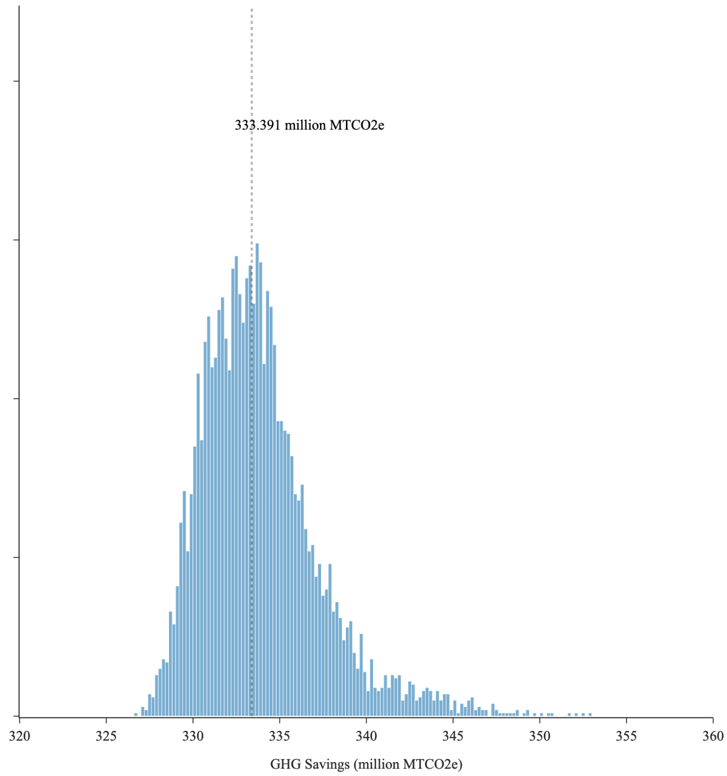

Figure B6. Distribution of 2035 total GHG reductions across model runs, Scenario 3

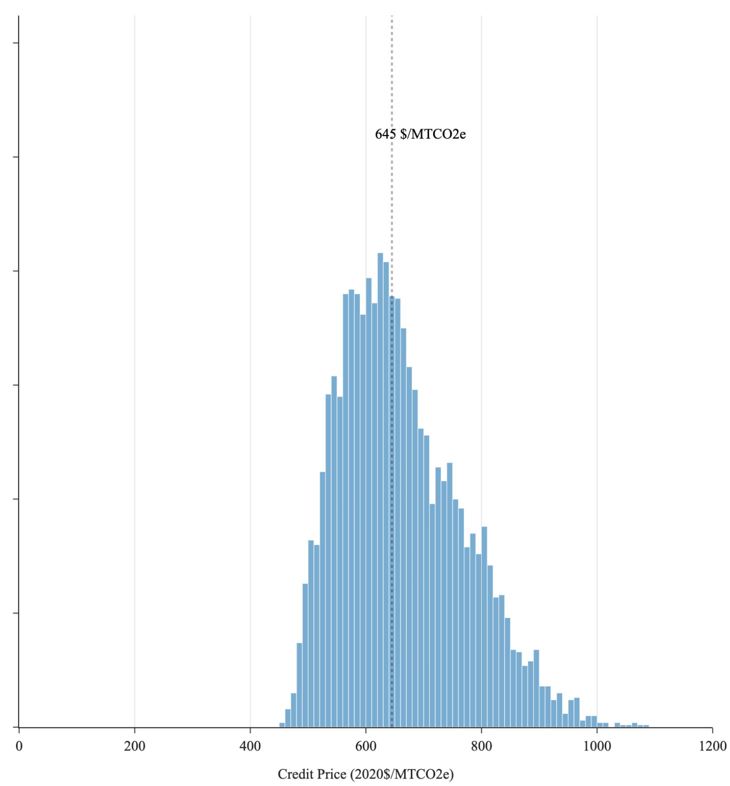

Figure B7. Distribution of 2035 LCFS credit prices across model runs, Scenario 4

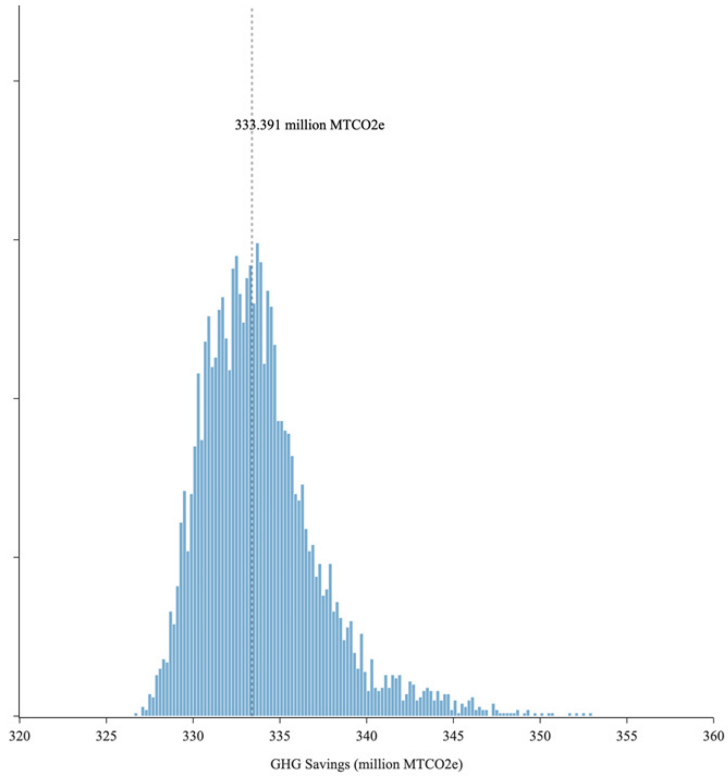

Figure B8. Distribution of 2035 total GHG reductions across model runs, Scenario 4

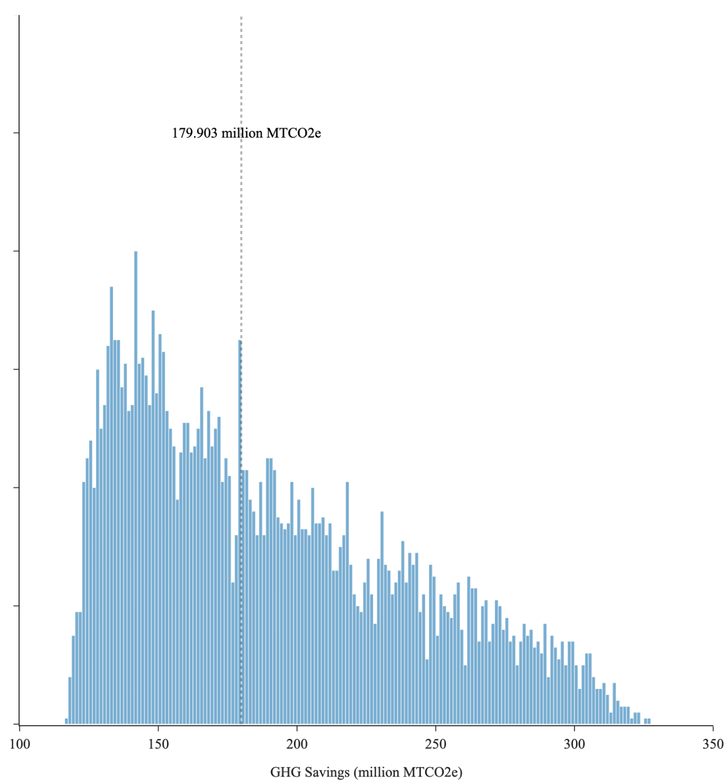

Figure B9. Distribution of 2035 total GHG reductions across model runs when factoring in post-hoc ILUC emissions adjustment, Scenario 4

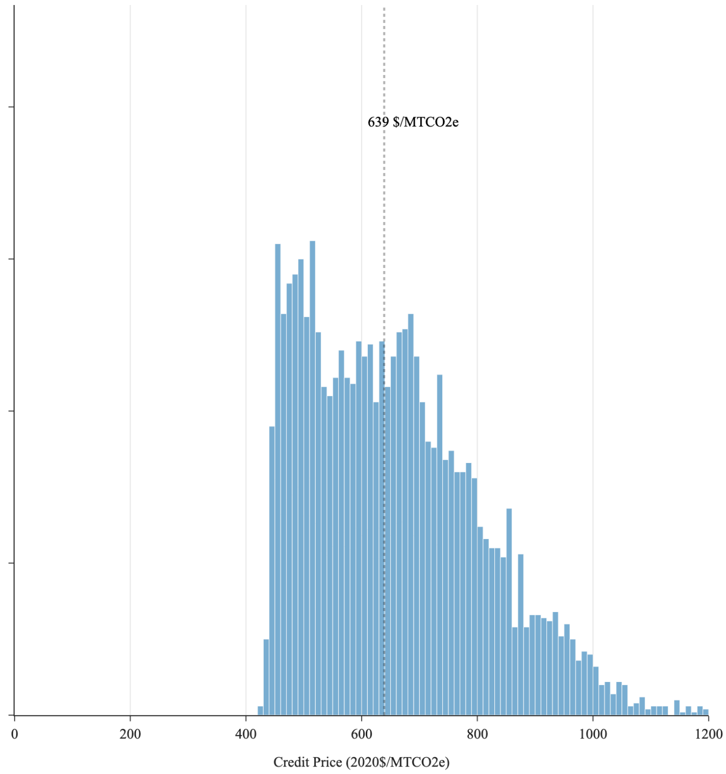

Figure B10. Distribution of 2035 LCFS credit prices across model runs, Scenario 5

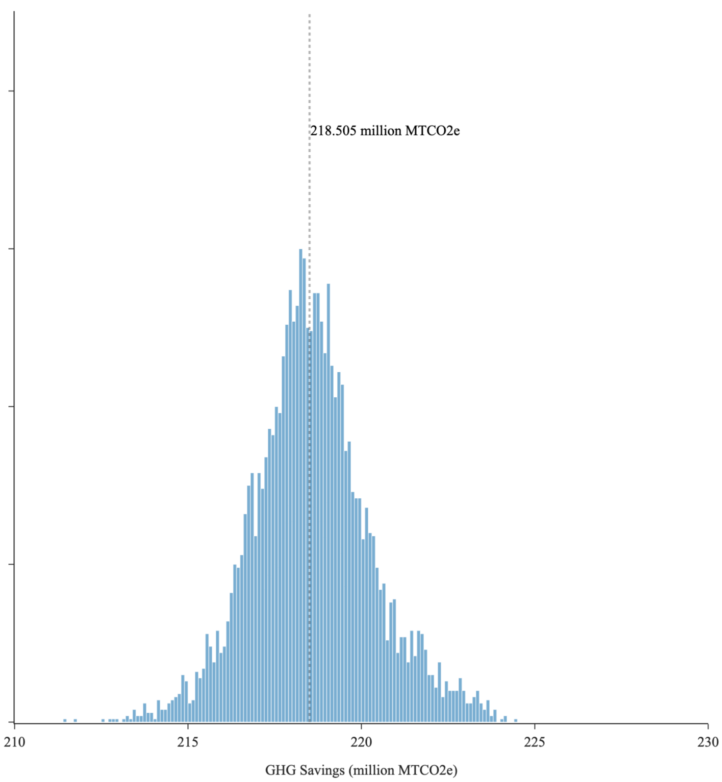

Figure B11. Distribution of 2035 total GHG reductions across model runs, Scenario 5

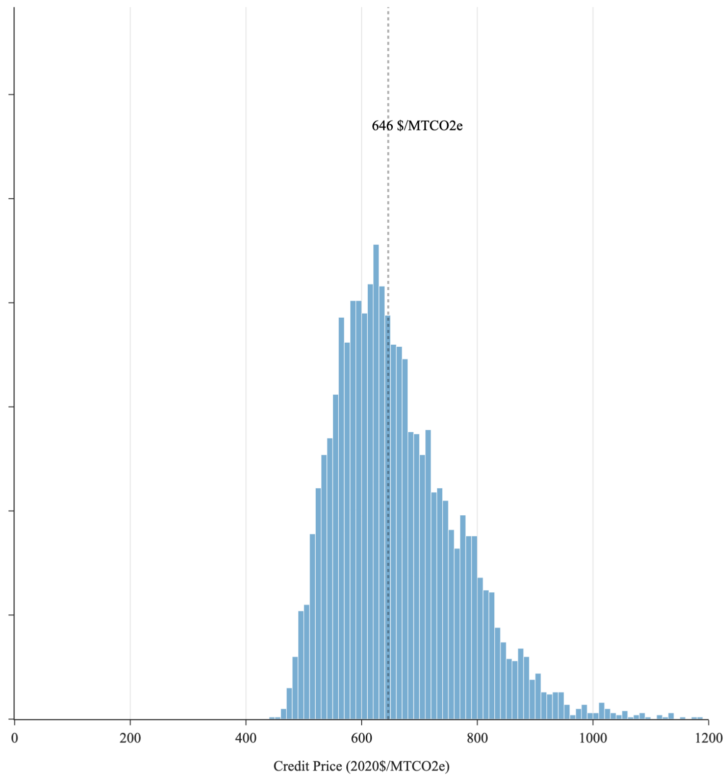

Figure B12. Distribution of 2035 LCFS credit prices across model runs, Scenario 6

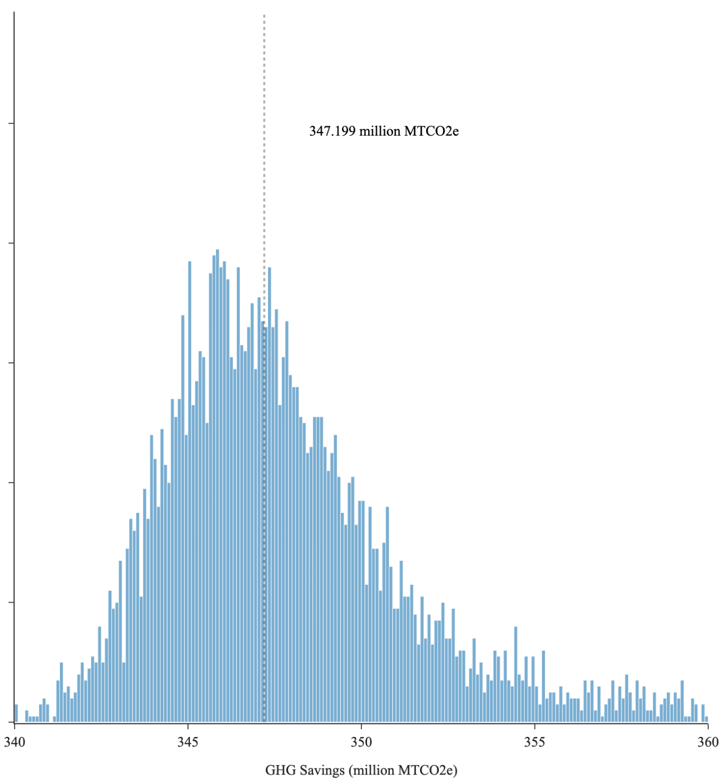

Figure B13. Distribution of 2035 total GHG reductions across model runs, Scenario 6

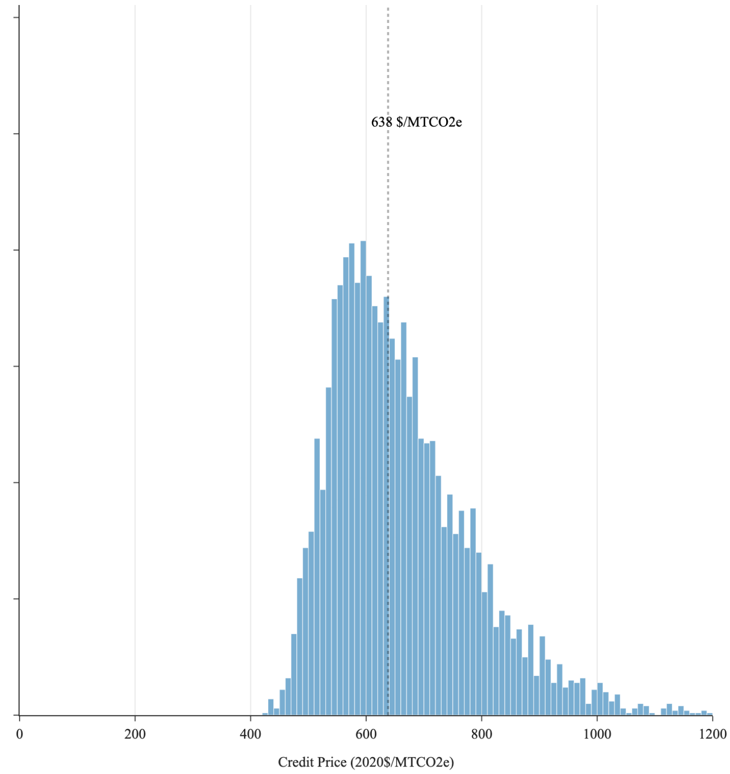

Figure B14. Distribution of 2035 LCFS credit prices across model runs, Scenario 7

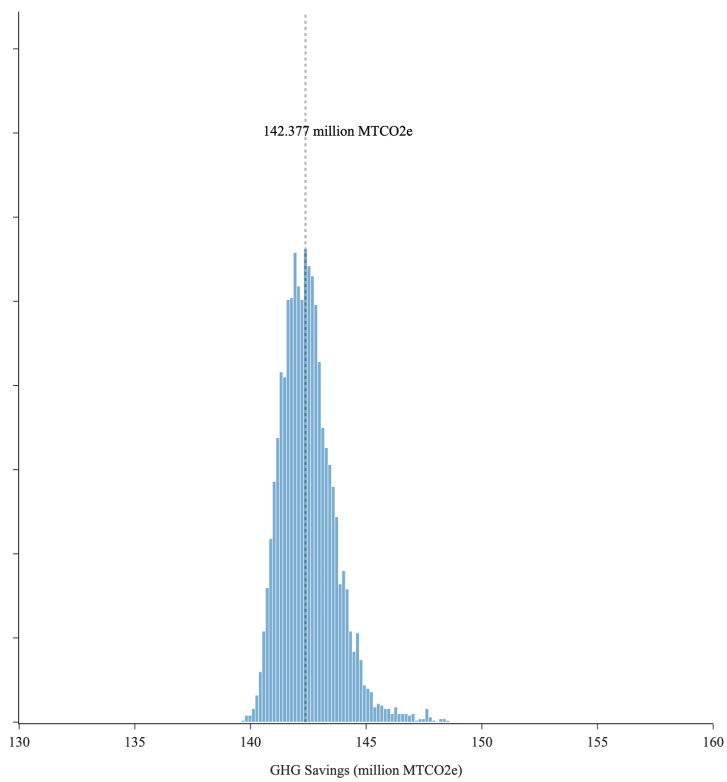

Figure B15. Distribution of 2035 total GHG reductions across model runs, Scenario 7

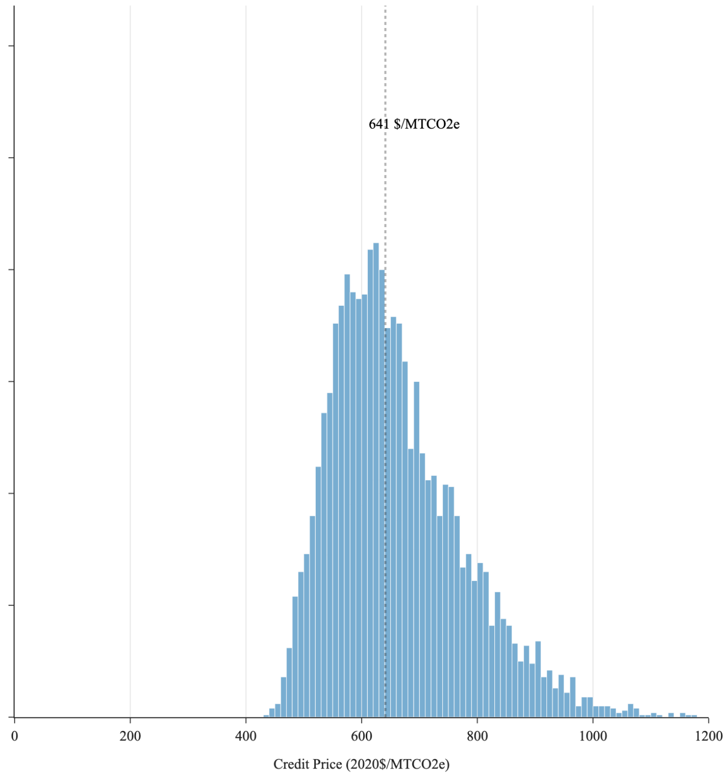

Figure B16. Distribution of 2035 LCFS credit prices across model runs, Scenario 8

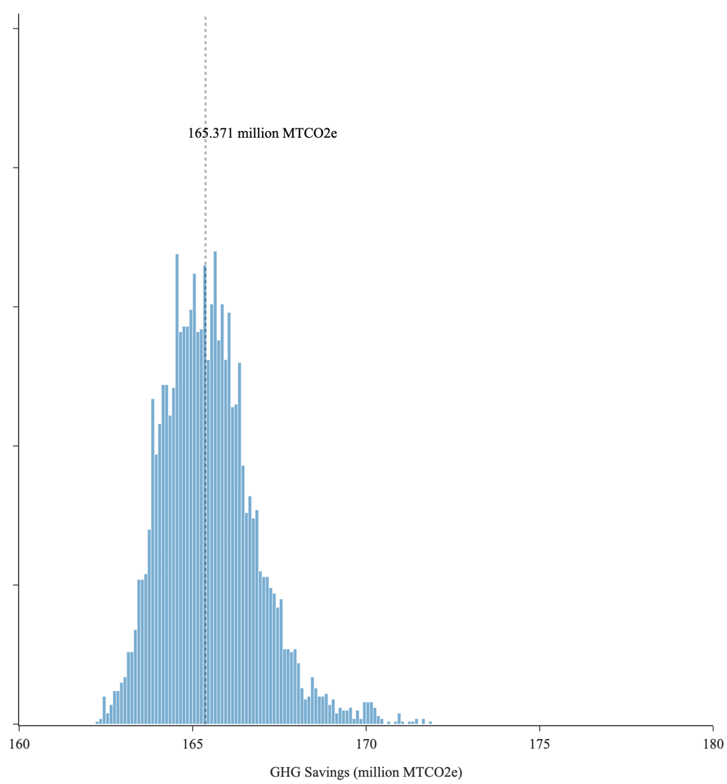

Figure B17. Distribution of 2035 total GHG reductions across model runs, Scenario 8

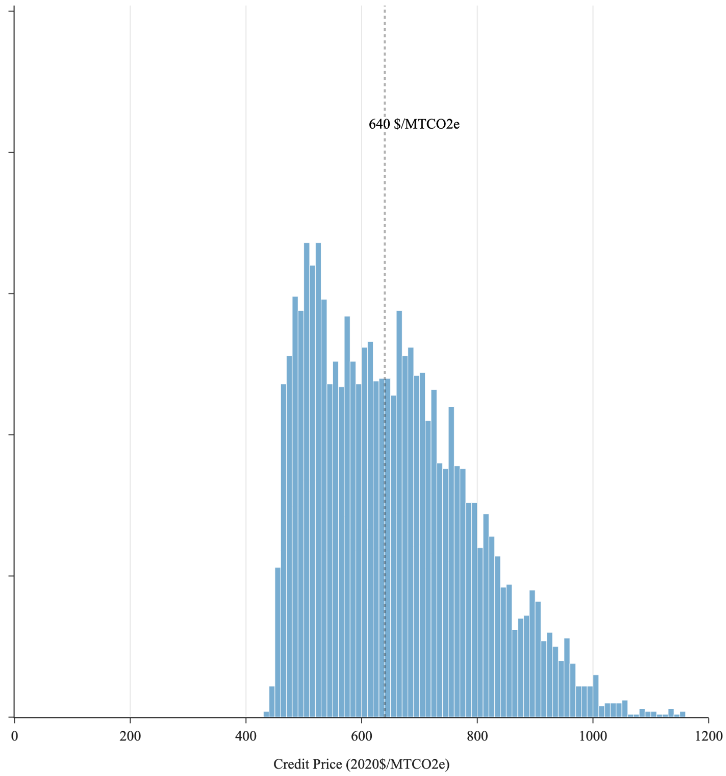

Figure B18. Distribution of 2035 LCFS credit prices across model runs, Scenario 9

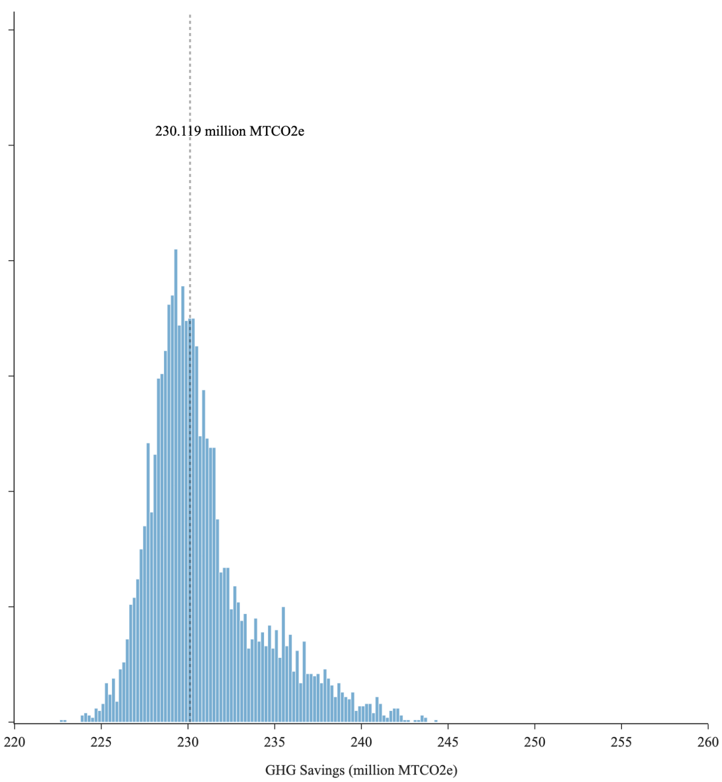

Figure B19. Distribution of 2035 total GHG reductions across model runs, Scenario 9